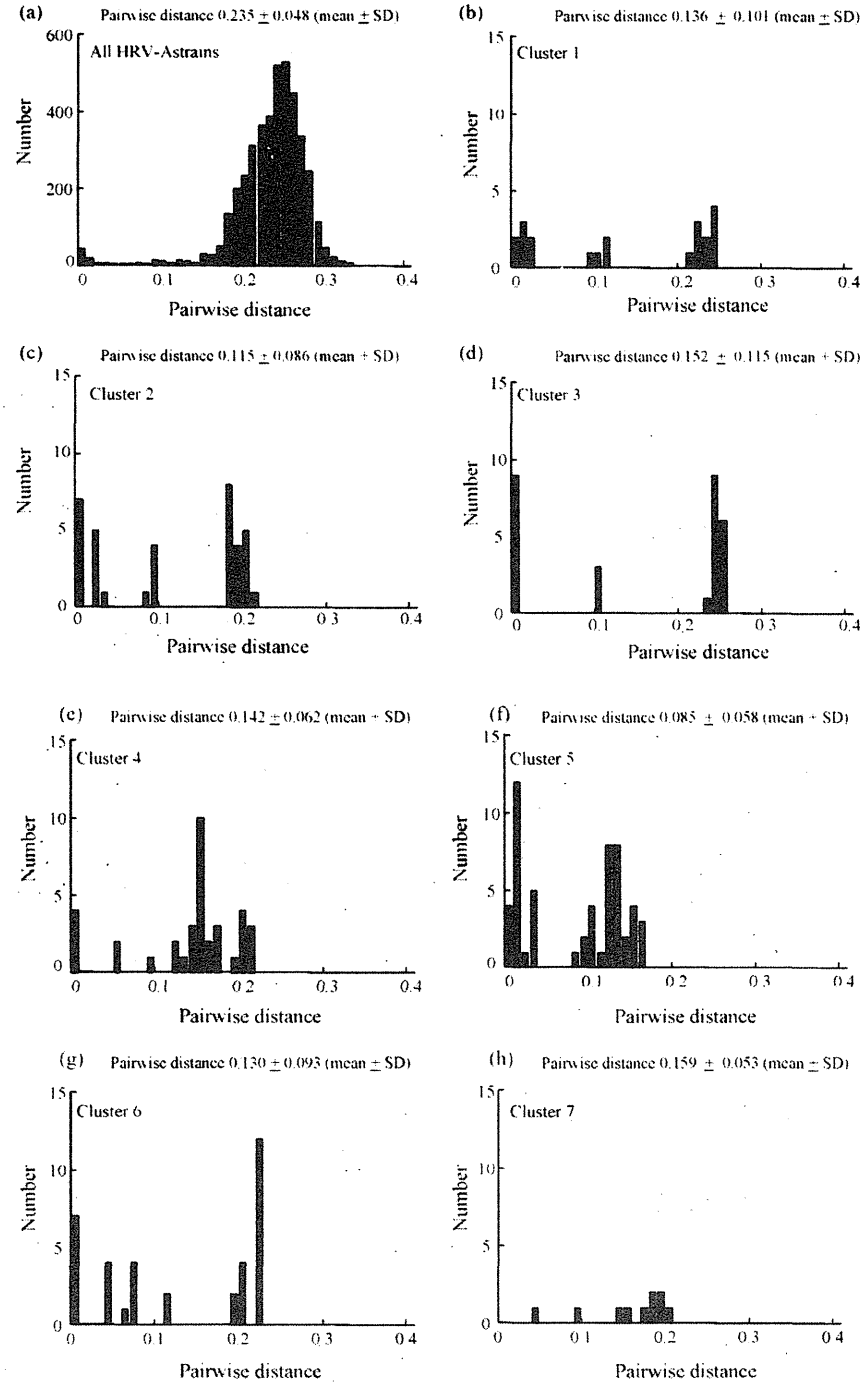

Fig. 2. Distributions of pairwise interspecies distances and pairwise distances for each intercluster for HRV-A based on nucleotide sequences of *VP4/VP2* coding region (390 nt). (a) Distribution of pairwise interspecies distances based on nucleotide sequences of the *VP4/VP2* coding region. (b–l) Distributions of pairwise distances for each intercluster (Clusters 1–11).

4. Discussion

To ascertain the address molecular epidemiology of domestic HRV-A infection, we performed phylogenetic and cluster analysis of the *VP4/VP2* coding region of prevalent strains (76 isolates) isolated from children with ARI in Yamagata prefecture, Japan during the period 2003–2007. Phylogenetic analysis based on the nucleotide and deduced amino acid sequences showed that the present HRV-A strains were clearly classified into 11 and 8 clusters, respectively. These viruses showed more than 30% of nucleotide divergence of the *VP4/VP2* cording region. The findings suggest that HRV-A with a wide genetic divergence was associated with URI and wheezy bronchiolitis during the investigation period in the study area.

Matsumoto et al. (1991) reported that approximately 32% of Japanese patients with ARI had associated HRV, although viruses were confirmed by a physicochemical method. Another study

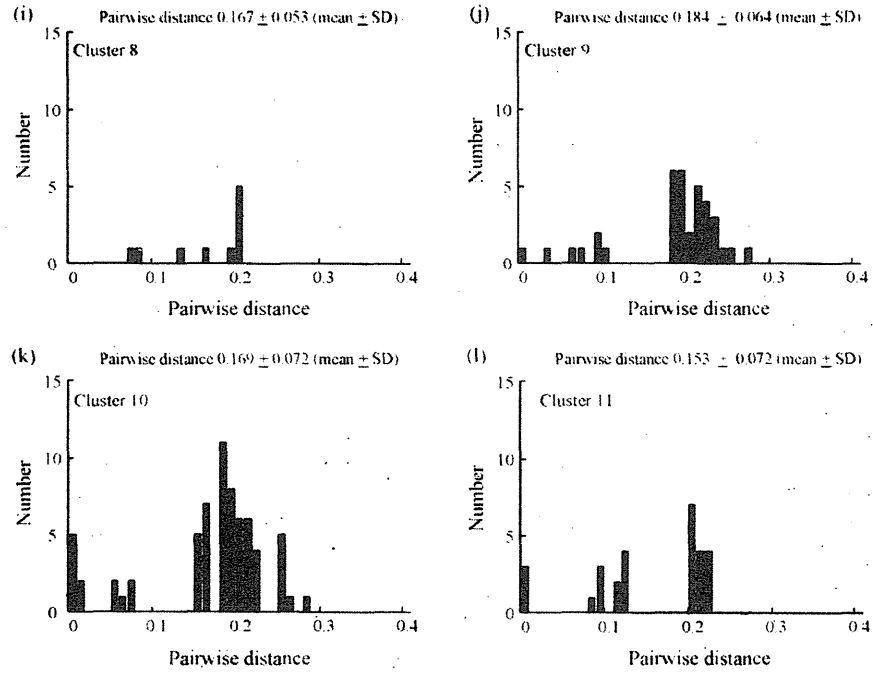

Fig. 2. (*Continued*).

found HRV in hospitalized infants with bronchiolitis and wheezing (Jartti et al., 2009). Calvo et al. (2007) reported that 25% of hospitalized infants with ARI had HRV infection as confirmed by multiplex PCR. In addition, HRV infections are frequently found in patients hospitalized with pneumonia (Cheuk et al., 2007). Savolainen et al. (2002a) showed that some serotypes of HRV, including HRV45, 78, and 81, were frequently associated with ARI in Finland. In American children with wheezing, various serotypes of HRV, including HRV30, 44, and 49, were found (Khetsuriani et al., 2008). In the present study, approximately 90% of patients with ARI had URI, and approximately 10% had wheezy bronchiolitis. Recent studies have shown that HRV can be classified into several species (Savolainen et al., 2002a,b). Savolainen et al. (2002b) reported that 61 isolates from patients with ARI could be classified into genetic groups 1 and 2, and these genetic groups could be further categorized into 12 clusters. Relations between genetic and serologic HRV type have been studied (Savolainen et al., 2002a). Most prototype HRV strains (isolates) have been classified into 2 species (HRV-A and -B). Of them, viruses belonging to species HRV-A comprise the major agent associated with ARI (Savolainen et al., 2002a). HRV-A can be subclassified into various clusters (Savolainen et al., 2002a). For example, McErlean reported that frequently detected HRV strains can be classified into 3 genotypes (Types A1, A2, and B) (McErlean et al., 2007). However, the detailed molecular epidemiology of HRV is not known. Moreover, to the best of our knowledge, there have been few molecular epidemiologic studies of HRV-A in Asian countries including Japan. Therefore, we performed a detailed phylogenetic and cluster analysis of HRV-A of patients with ARI, such as upper respiratory infections and wheezy bronchiolitis, in Yamagata prefecture, Japan. We found that prevalent HRV-A strains isolated from Japanese patients with ARI showed a wide nucleotide divergence. The data suggested that HRV-A strains belonging to some clusters were associated with wheezy bronchiolitis. However, we do not know whether these viruses can easily cause wheezy bronchiolitis because only 6 cases of wheezy bronchiolitis caused by HRV-A were examined in the present study. Recent evidence suggests that some genotypes of respiratory viruses, such as HRV, respiratory syncytial virus (RSV), and parainfluenza viruses, may be linked to virus-induced asthma (Jartti et al., 2004, 2007; Martinello et al., 2002). For example, a specific genotype (GA 3) of RSV may be associated with significantly greater severity of illness (Martinello et al., 2002). However, another report showed no association between severity of illness and RSV subgroups, and the severity was instead associated with the amount of RSV in nasopharyngial aspirates (Campanini et al., 2007; Sato et al., 2005). Thus, the association between a specific virus type and the severity of RSV infections, including bronchiolitis, has not been precisely addressed. In addition, Johnston (2007) reported that HRV infection is strongly related to virus-induced asthma or exacerbation of asthma. As possible reason for this association with HRV-induced asthma is insufficient production of the cytokine interferon-β or λ; however, the molecular mechanisms underlying this are not fully understood as yet (Johnston, 2007). Additional studies with large numbers of patients with HRV-induced airway hyperresponsiveness, including asthma, would be beneficial.

The *VP4/VP2* coding region encodes interior viral capsid. Genetic clustering on the basis of the *VP4/VP2* sequences was reported to be an effective method for the identification of many types of HRV isolates (Savolainen et al., 2002a). To better perform phylogenetic and cluster analysis of many types of HRV-A in the present study, we selected the *VP4/VP2* coding region, which resulted in the construction of a clearly distinguishable phylogenetic tree (Savolainen et al., 2002a; Kiang et al., 2007). Thus, the use of this coding region for phylogenetic analysis of HRV may be suitable for the clustering of many field isolates of HRV, consistent with earlier reports (Savolainen et al., 2002a,b).

We were able to collect clinical specimens from only a relatively small number of pediatric patients with ARI in a limited area (Yamagata prefecture), covering only a small number of HRV-A strains from children who attended a pediatric clinic. In addition, no seasonal variation of HRV was found in the present data, but it may be important to address seasonal variation regarding HRV epidemiology as a future research topic. To address the

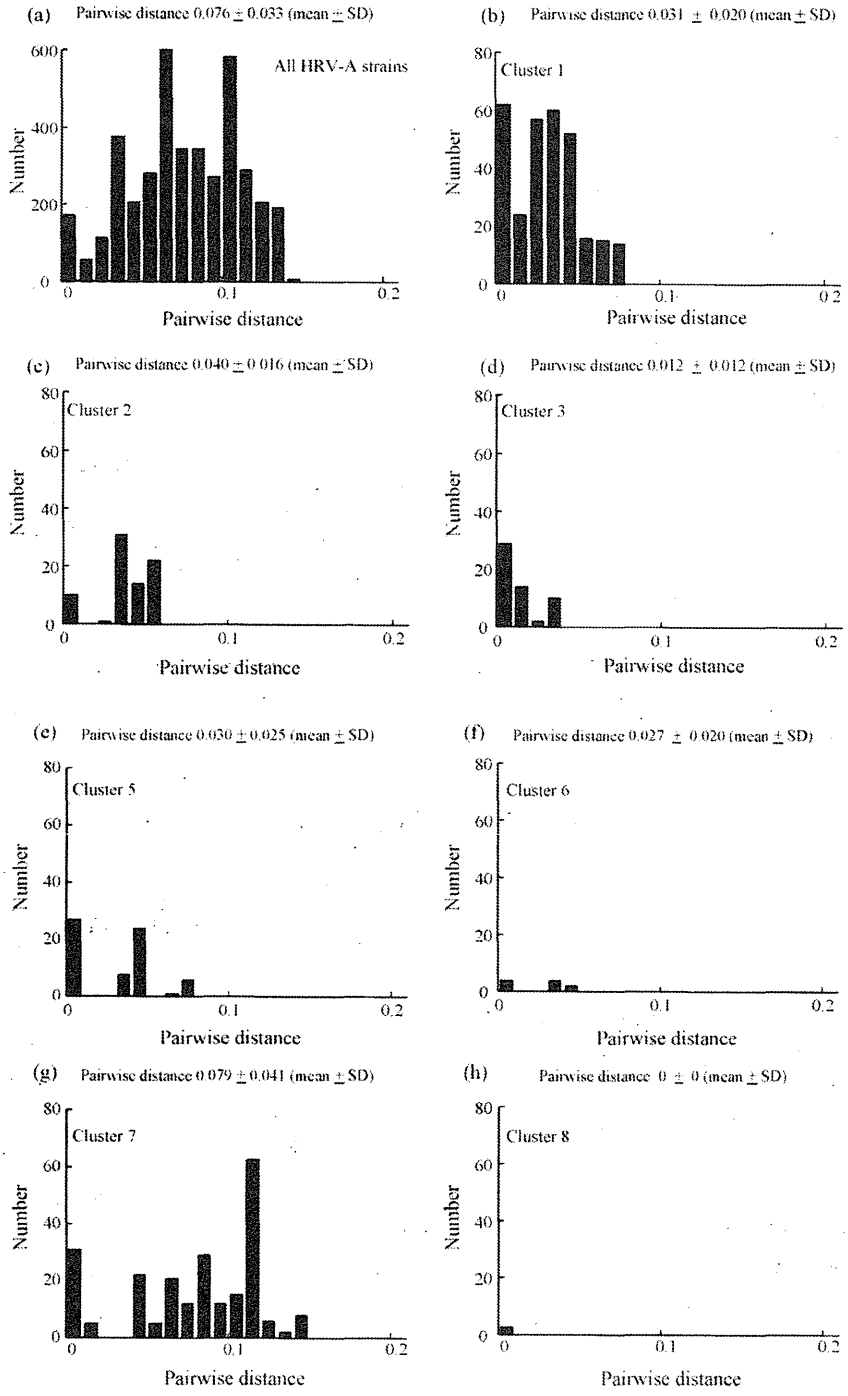

Fig. 3. Distributions of pairwise interspecies distances and pairwise distances for each intercluster for HRV-A based on deduced amino acid sequences of *VP4/VP2* coding region (130 aa). (a) Distribution of pairwise interspecies distances based on amino acid sequences of the *VP4/VP2* coding region. (b–h) Distributions of pairwise distances for each intercluster (Clusters 1–3 and 5–8).

domestic epidemiology of HRV more comprehensively large numbers of HRV strains derived from adults and large areas will be required.

In conclusion, various genetic types of HRV-A appear to be associated with ARI, including URI and wheezy bronchiolitis, in Japanese children. Further molecular epidemiologic investigations regarding the other HRV species (HRV-B and HRV-C) should be performed.

Acknowledgements

We thank Drs. Kazushi Motomura and Hironori Sato (Center for Pathogen Genomics, National Institute of Infectious Diseases, Japan) for helpful discussions. This work was supported in part by Research on Emerging and Re-emerging Infectious Diseases, Labour, and Welfare Programs from the Ministry of Health, Labour, and Welfare, Japan (No. 24-19211301).

References

Campanini, G., Percivalle, E., Baldanti, F., Rovida, F., Bertaina, A., Marchi, A., Stronati, M., Gerna, G., 2007. Human respiratory syncytial virus (hRSV) RNA quantification in nasopharyngeal secretions identifies the hRSV etiologic role in acute respiratory tract infections of hospitalized infants. J. Clin. Virol. 39, 119–124.

Calvo, C., García-García, M.L., Blanco, C., Pozo, F., Flecha, I.C., Pérez-Breña, P., 2007. Role of rhinovirus in hospitalized infants with respiratory tract infections in Spain. Pediatr. Infect. Dis. J. 26, 904–908.

Cherry, J.D., 2003. The Common Cold. In: Feigin, R.D., Cherry, J.D., Demmler, G.J., Kaplan, S.L. (Eds.), Textbook of Pediatric Infectious Diseases, fifth ed. Saunders, Philadelphia, pp. 140–146.

Cheuk, D.K., Tang, I.W., Chan, K.H., Woo, P.C., Peiris, M.J., Chiu, S.S., 2007. Rhinovirus infection in hospitalized children in Hong Kong: a prospective study. Pediatr. Infect. Dis. J. 26, 995–1000.

Imakita, M., Shiraki, K., Yutani, C., Ishibashi-Ueda, H., 2000. Pneumonia caused by rhinovirus. Clin. Infect. Dis. 30, 611–612.

Iwai, M., Yoshida, H., Matsuura, K., Fujimoto, T., Shimizu, H., Takizawa, T., Nagai, Y., 2006. Molecular epidemiology of echoviruses 11 and 13, based on an environmental surveillance conducted in Toyama Prefecture, 2002–2003. Appl. Environ. Microbiol. 72, 6381–6387.

Jackson, D.J., Gangnon, R.E., Evans, M.D., Roberg, K.A., Anderson, E.L., Pappas, T.E., Printz, M.C., Lee, W.M., Shult, P.A., Reisdorf, E., Carlson-Dakes, K.T., Salazar, L.P., DaSilva, D.F., Tisler, C.J., Gern, J.E., Lemanske Jr., R.F., 2008. Wheezing rhinovirus illnesses in early life predict asthma development in high-risk children. Am. J. Respir. Crit. Care Med. 178, 667–672.

Jartti, T., Lehtinen, P., Vuorinen, T., Osterback, R., van den Hoogen, B., Osterhaus, A.D., Ruuskanen, O., 2004. Respiratory picornaviruses and respiratory syncytial virus as causative agents of acute expiratory wheezing in children. Emerg. Infect. Dis. 10, 1095–1101.

Jartti, T., Lehtinen, P., Vuorinen, T., Ruuskanen, O., 2009. Bronchiolitis: age and previous wheezing episodes are linked to viral etiology and atopic characteristics. Pediatr. Infect. Dis. J. 28, 311–317.

Jartti, T., Waris, M., Niesters, H.G., Allander, T., Ruuskanen, O., 2007. Respiratory viruses and acute asthma in children. J. Allergy Clin. Immunol. 120, 216.

Johnston, S.L., 2007. Innate immunity in the pathogenesis of virus-induced asthma exacerbations. Proc. Am. Thorac. Soc. 4, 267–270.

Johnston, S.L., Pattemore, P.K., Sanderson, G., Smith, S., Campbell, M.J., Josephs, L.K., Cunningham, A., Robinson, B.S., Myint, S.H., Ward, M.E., Tyrrell, D.A., Holgate, S.T., 1996. The relationship between upper respiratory infections and hospital admissions for asthma: a time-trend analysis. Am. J. Respir. Crit. Care Med. 154, 654–660.

Katayama, K., Shirato-Horikoshi, H., Kojima, S., Kageyama, T., Oka, T., Hoshino, F., Fukushi, S., Shinohara, M., Uchida, K., Suzuki, Y., Gojobori, T., Takeda, N., 2002. Phylogenetic analysis of the complete genome of 18 Norwalk-like viruses. Virology 299, 225–239.

Khetsuriani, N., Lu, X., Teague, W.G., Kazerouni, N., Anderson, L.J., Erdman, D.D., 2008. Novel human rhinoviruses and exacerbation of asthma in children. Emerg. Infect. Dis. 14, 1793–1796.

Kiang, D., Yagi, S., Kantardjieff, K.A., Kim, E.J., Louie, J.K., Schnurr, D.P., 2007. Molecular characterization of a variant rhinovirus from an outbreak associated with uncommonly high mortality. J. Clin. Virol. 38, 227–237.

Kimura, M., 1980. A simple method for estimating evolutionary rates of base substitutions through comparative studies of nucleotide sequences. J. Mol. Evol. 16, 111–120.

Lau, S.K., Yip, C.C., Tsoi, H.W., Lee, R.A., So, L.Y., Lau, Y.L., Chan, K.H., Woo, P.C., Yuen, K.Y., 2007. Clinical features and complete genome characterization of a distinct human rhinovirus (HRV) genetic cluster, probably representing a previously undetected HRV species, HRV-C, associated with acute respiratory illness in children. J. Clin. Microbiol. 45, 3655–3664.

Martinello, R.A., Chen, M.D., Weibel, C., Kahn, J.S., 2002. Correlation between respiratory syncytial virus genotype and severity of illness. J. Infect. Dis. 186, 839–842.

Matsumoto, I., Yoshida, S., Takahashi, K., Kawana, R., 1991. Virological surveillance of acute respiratory tract illnesses of children in Morioka, Japan. I. Epidemiological patterns of infection with respiratory viruses over a 10-year period. Kansenshogaku Zasshi 65, 423–432.

McErlean, P., Shackelton, L.A., Lambert, S.B., Nissen, M.D., Sloots, T.P., Mackay, I.M., 2007. Characterisation of a newly identified human rhinovirus, HRV-QPM, discovered in infants with bronchiolitis. J. Clin. Virol. 39, 67–75.

Mizuta, K., Abiko, C., Aoki, Y., Suto, A., Hoshina, H., Itagaki, T., Katsushima, N., Matsuzaki, Y., Hongo, S., Noda, M., Kimura, H., Ootani, K., 2008. Analysis of monthly isolation of respiratory viruses from children by cell culture using a microplate method: a two-year study from 2004 to 2005 in Yamagata, Japan. Jpn. J. Infect. Dis. 61, 196–201.

Nicholson, K.G., Kent, J., Ireland, D.C., 1993. Respiratory viruses and exacerbations of asthma in adults. BMJ 307, 982–986.

Papadopoulos, N.G., Moustaki, M., Tsolia, M., Bossios, A., Astra, E., Prezerakou, A., Gourgiotis, D., Kafetzis, D., 2002. Association of rhinovirus infection with increased disease severity in acute bronchiolitis. Am. J. Respir. Crit. Care Med. 165, 1285–1289.

Piralla, A., Rovida, F., Campanini, G., Rognoni, V., Marchi, A., Locatelli, F., Gerna, G., 2009. Clinical severity and molecular typing of human rhinovirus C strains during a fall outbreak affecting hospitalized patients. J. Clin. Virol. 45, 311–317.

Robert, C.W., 2003. Bronchiolitis and Infectious Asthma. In: Feigin, R.D., Cherry, J.D., Demmler, G.J., Kaplan, S.L. (Eds.), Textbook of Pediatric Infectious Diseases, fifth ed. Saunders, Philadelphia, pp. 273–282.

Saitou, N., Nei, M., 1987. The neighbor-joining method: a new method for reconstructing phylogenetic trees. Mol. Biol. Evol. 4, 406–425.

Sato, M., Saito, R., Sakai, T., Sano, Y., Nishikawa, M., Sasaki, A., Shobugawa, Y., Gejyo, F., Suzuki, H., 2005. Molecular epidemiology of respiratory syncytial virus infections among children with acute respiratory symptoms in a community over three seasons. J. Clin. Microbiol. 43, 36–40.

Savolainen, C., Blomqvist, S., Mulders, M.N., Hovi, T., 2002a. Genetic clustering of all 102 human rhinovirus prototype strains: serotype 87 is close to human enterovirus 70. J. Gen. Virol. 83, 333–340.

Savolainen, C., Mulders, M.N., Hovi, T., 2002b. Phylogenetic analysis of rhinovirus isolates collected during successive epidemic seasons. Virus Res. 85, 41–46.

Turner, R.B., Couch, R.B., 2007. Rhinovirus. In: Knipe, D.M., Hawley, P.M. (Eds.), Fields Virology, fifth ed. Lippincott Williams & Wilkins, Philadelphia, PA, pp. 895–909.

Wos, M., Sanak, M., Soja, J., Olechnowicz, H., Busse, W.W., Szczeklik, A., 2008. The presence of rhinovirus in lower airways of patients with bronchial asthma. Am. J. Respir. Crit. Care Med. 177, 1082–1089.

Journal of Virology

HIV-1 Infection *Ex Vivo* Accelerates Measles Virus Infection by Upregulating Signaling Lymphocytic Activation Molecule (SLAM) in CD4 $^{+}$ T Cells

Yu-ya Mitsuki, Kazutaka Terahara, Kentaro Shibusawa, Takuya Yamamoto, Takatsugu Tsuchiya, Fuminori Mizukoshi, Masayuki Ishige, Seiji Okada, Kazuo Kobayashi, Yuko Morikawa, Tetsuo Nakayama, Makoto Takeda, Yusuke Yanagi and Yasuko Tsunetsugu-Yokota

***J. Virol.* 2012, 86(13):7227. DOI: 10.1128/JVI.06681-11.**
Published Ahead of Print 24 April 2012.

Updated information and services can be found at:
http://jvi.asm.org/content/86/13/7227

These include:

SUPPLEMENTAL MATERIAL Supplemental material

REFERENCES This article cites 29 articles, 19 of which can be accessed free at: http://jvi.asm.org/content/86/13/7227#ref-list-1

CONTENT ALERTS Receive: RSS Feeds, eTOCs, free email alerts (when new articles cite this article), more»

Information about commercial reprint orders: **http://journals.asm.org/site/misc/reprints.xhtml**
To subscribe to to another ASM Journal go to: **http://journals.asm.org/site/subscriptions/**

Journals.ASM.org

Downloaded from http://jvi.asm.org/ on January 30, 2013 by Natinoal Institute of Infectius Diseases, Murayama Bunshitsu

JVI
Journals.ASM.org

HIV-1 Infection *Ex Vivo* Accelerates Measles Virus Infection by Upregulating Signaling Lymphocytic Activation Molecule (SLAM) in $CD4^+$ T Cells

Yu-ya Mitsuki,[a] Kazutaka Terahara,[a] Kentaro Shibusawa,[a] Takuya Yamamoto,[b] Takatsugu Tsuchiya,[a] Fuminori Mizukoshi,[a] Masayuki Ishige,[a,c] Seiji Okada,[c] Kazuo Kobayashi,[a] Yuko Morikawa,[d] Tetsuo Nakayama,[e] Makoto Takeda,[f] Yusuke Yanagi,[g] and Yasuko Tsunetsugu-Yokota[a]

Department of Immunology, National Institute of Infectious Diseases, Shinjuku-ku, Tokyo, Japan[a]; Immunology Laboratory, Vaccine Research Center, National Institute of Allergy and Infectious Diseases, National Institutes of Health, Bethesda, Maryland, USA[b]; Center for AIDS Research, Kumamoto University, Kumamoto, Japan[c]; Laboratory of Viral Infection II, Kitasato Institute for Life Science, Kitasato University, Tokyo, Japan[d]; Laboratory of Viral Infection I, Kitasato Institute for Life Science, Kitasato University, Tokyo, Japan[e]; Department of Virology III, National Institute of Infectious Diseases, Tokyo, Japan[f]; and Department of Virology, Faculty of Medicine, Kyushu University, Fukuoka, Japan[g]

Measles virus (MV) infection in children harboring human immunodeficiency virus type 1 (HIV-1) is often fatal, even in the presence of neutralizing antibodies; however, the underlying mechanisms are unclear. Therefore, the aim of the present study was to examine the interaction between HIV-1 and wild-type MV (MVwt) or an MV vaccine strain (MVvac) during dual infection. The results showed that the frequencies of MVwt- and MVvac-infected $CD4^+$ T cells within the resting peripheral blood mononuclear cells (PBMCs) were increased 3- to 4-fold after HIV-1 infection, and this was associated with a marked upregulation of signaling lymphocytic activation molecule (SLAM) expression on $CD4^+$ T cells but not on $CD8^+$ T cells. SLAM upregulation was induced by infection with a replication-competent HIV-1 isolate comprising both the X4 and R5 types and to a lesser extent by a pseudotyped HIV-1 infection. Notably, SLAM upregulation was observed in HIV-infected as well as -uninfected $CD4^+$ T cells and was abrogated by the removal of HLA-DR^+ cells from the PBMC culture. Furthermore, SLAM upregulation did not occur in uninfected PBMCs cultured together with HIV-infected PBMCs in compartments separated by a permeable membrane, indicating that no soluble factors were involved. Rather, $CD4^+$ T cell activation mediated through direct contact with dendritic cells via leukocyte function-associated molecule 1 (LFA-1)/intercellular adhesion molecule 1 (ICAM-1) and LFA-3/CD2 was critical. Thus, HIV-1 infection induces a high level of SLAM expression on $CD4^+$ T cells, which may enhance their susceptibility to MV and exacerbate measles in coinfected individuals.

The attenuated measles virus (MV) vaccine has greatly reduced the morbidity and mortality of measles in industrialized countries. However, measles is still a leading cause of death among children in developing countries, especially in sub-Saharan Africa, where almost 90% of global pediatric human immunodeficiency virus type 1 (HIV-1) infections occur (http://apps.who.int/ghodata/). Because both HIV-1 and MV cause immunosuppression, it is conceivable that coinfection with HIV-1 and MV increases the risk of disease progression (17). In fact, an observational study of hospitalized children in Zambia showed that the fatality rate increased among HIV-1-infected children with measles (18).

The low levels of neutralizing antibodies in HIV-1-infected children may explain the high mortality of measles. The measles vaccine is only weakly immunogenic in HIV-1-infected children, inducing only low levels of neutralizing antibody, which decline rapidly (17). However, a recent large-scale prospective study in Zambia conducted by Moss et al. reported a good initial antibody response to measles vaccine in both HIV-1-infected and -uninfected children (19). Moreover, to understand the impact of HIV-1 infection on the clinical manifestation of measles, Permar et al. conducted a study using MV-vaccinated or -unvaccinated rhesus monkeys that are chronically infected with a simian immunodeficiency virus (24). They monitored the virological and immunological status of the monkeys after MV challenge and found that the clinical manifestation of measles occurs even in monkeys with high titers of vaccine-induced MV neutralizing antibody. This finding implies that the presence of neutralizing antibody alone is not sufficient protection from measles in HIV-1-infected individuals. Therefore, it is highly likely that an as yet unknown factor(s)/mechanism(s) affected by HIV-1 is involved in the exacerbation of measles in HIV-1-infected individuals.

Some studies analyzed the interaction between MV and HIV-1 *in vitro*. Garcia et al. studied HIV-1 replication in peripheral blood mononuclear cells (PBMCs) coinfected with MV and found that MV-induced inhibition of lymphocyte proliferation suppresses HIV-1 replication, but without any apparent increase in the production of chemokines or any other soluble factors in coinfected cultures (7). In a more recent study, the same group demonstrated that the cell cycle progression of T cells, which is required for efficient HIV-1 replication, was blocked by MV (8); however, it is still not clear whether HIV-1 affects MV infection directly or indirectly.

Understanding the impact of HIV-1 infection on MV infection

Received 28 October 2011 Accepted 10 April 2012
Published ahead of print 24 April 2012
Address correspondence to Yasuko Tsunetsugu-Yokota, yyokota@nih.go.jp.
Supplemental material for this article may be found at http://jvi.asm.org/.
Copyright © 2012, American Society for Microbiology. All Rights Reserved.
doi:10.1128/JVI.06681-11

Downloaded from http://jvi.asm.org/ on January 30, 2013 by National Institute of Infectious Diseases, Murayama Bunshitsu

and replication is important both for developing successful strategies for measles eradication and for HIV-1 control. The receptor for wild-type MV has been identified to be signaling lymphocytic activation molecule (SLAM; also known as CD150), and attenuated vaccine strains can utilize both SLAM and CD46 (4). Recently, nectin4 was also identified as an MV receptor that is important for MV to spread into epithelial cells and release viral particles from the apical membrane into the lumen of the respiratory tract (20, 21). However, SLAM remains a major receptor of MV in lymphoid organs and plays an important role in a systemic MV infection. Therefore, the aim of the present study was to investigate the course of MV infection in HIV-1-infected PBMCs *ex vivo* at the level of the individual cell, focusing on SLAM expression. The results presented here showed that HIV-1 replication in resting PBMCs induces the upregulation of SLAM expression on $CD4^+$ T cells in a manner that is dependent on cell-to-cell contact, resulting in higher levels of MV infection.

MATERIALS AND METHODS

Cell preparation. Human peripheral blood samples were collected from healthy donors after receiving written informed consent. Sample collection was approved by the institutional ethical committee of the National Institute of Infectious Diseases (Tokyo, Japan). PBMCs were separated by Ficoll-Hypaque density gradient centrifugation (Lymphosepal; IBL, Gunma, Japan). T cells were isolated using a total T cell enrichment kit (StemCell Technologies, Vancouver, BC, Canada), after depletion of $CD14^+$ cells. For monocyte depletion, $CD14^+$ cells were depleted from PBMCs using magnetically activated cell sorting (MACS) with CD14 microbeads (Miltenyi Biotec, Cologne, Germany). For B cell and HLA-DR^+ cell depletion, PBMCs were incubated with biotin-labeled anti-CD19 (BioLegend, San Diego, CA) and biotin-labeled anti-HLA-DR (BioLegend) antibodies, respectively, followed by positive selection using anti-biotin tetrameric antibody complex (TAC), magnetic colloid, and an EasySep magnet (all from StemCell Technologies).

Preparation of virus stock. To prepare HIV-1 clones HIV-$1_{NL\text{-}E}$, HIV-$1_{NLAD8\text{-}E}$, and HIV-$1_{NL\text{-}D}$, human 293T embryonic kidney cells seeded at a density of 7×10^6 cells/15-cm dish were transfected with 30 μg of pNL-E, pNLAD8-E, and pNL-D, respectively, using the calcium phosphate precipitation method as described previously (29). To prepare HIV-1 pseudotyped with vesicular stomatitis virus glycoprotein (HIV-1/VSV-G), 293T cells were cotransfected with 36 μg of pNL-EdENV (pNL-E with an *env*-inactivating mutation) and 4 μg of pVSV-G per 7×10^6 cells. At 2 days posttransfection, the culture supernatant was collected, filtrated, and frozen at −80°C. The amounts of viruses in each culture supernatant were measured using an in-house HIV-1 Gag p24 enzyme-linked immunosorbent assay.

To prepare green fluorescent protein (GFP)-expressing wild-type (IC323-EGFP) (12) or vaccine strain (GFP-MVAIK) (6) MV, 1×10^7 human SLAM-expressing Vero cells (Vero/hSLAM) cells were infected with 1×10^5 PFU of each virus (multiplicity of infection [MOI] = 0.01) for 2 h, washed, and then grown in Dulbecco's modified Eagle medium (DMEM; Gibco, Carlsbad, CA) supplemented with 2% heat-inactivated fetal bovine serum (FBS). Infected cells were harvested when approximately 80% cytotoxicity was observed. Cells were then frozen and thawed three times and sonicated for 10 s to release the cell-bound viruses. The titer of measles virus was measured using a plaque assay, described in the following section.

Titration of MV. MV was titrated as described previously (26). In brief, monolayers of 2×10^5 Vero/hSLAM cells grown in 12-well plates were infected with serially diluted wild-type MV (MVwt) or an attenuated MV vaccine strain (MVvac). After removal of viruses, the cells were overlaid with DMEM supplemented with 2% methylcellulose and 2% FBS. At day 5 postinfection, cells were stained with 5% neutral red, the numbers of plaques were counted, and the numbers of PFU/ml were calculated.

HIV-1 and MV infection. For HIV-1 infection, untreated PBMCs or PBMCs depleted of either $CD14^+$ monocytes, $CD19^+$ B cells, or HLA-DR^+ cells or purified T cells (1×10^6 cells) were infected with 100 ng of p24 of either HIV-$1_{NL\text{-}E}$, HIV-$1_{NL\text{-}D}$, HIV-$1_{NLAD8\text{-}E}$, or HIV-1/VSV-G for 2 h, washed three times with RPMI 1640 (RPMI), and then cultured in RPMI supplemented with 5% heat-inactivated human serum (P-RPMI), penicillin (100 μg/ml), and streptomycin (100 μg/ml). At day 3 postinfection, the culture medium was changed to 5% P-RPMI supplemented with interleukin-2 (IL-2; 50 U/ml) and then cultured for 2 days.

For MV infection, HIV-$1_{NL\text{-}D}$-infected and -uninfected PBMCs (1×10^6 cells) were mock infected or infected with 5×10^4 PFU of either MVwt or MVvac for 2 h at day 5 after HIV infection, washed three times with RPMI, and then cultured in 5% P-RPMI for 2 days.

Flow cytometry. Cells were stained with a suitable combination of fluorescence-labeled monoclonal antibodies (MAbs): Pacific Blue-labeled anti-CD4 (eBioscience, San Diego, CA), allophycocyanin (APC)-Cy7-labeled anti-CD8 (eBioscience), peridinin chlorophyll protein-labeled anti-CD3 (R&D Systems, Inc., Minneapolis, MN), APC-labeled anti-CD14 (R&D Systems), phycoerythrin (PE)-labeled anti-SLAM (eBioscience), and PE-Cy7-labeled anti-CD19 (BioLegend). Dead cells were visualized using a LIVE/DEAD fixable dead cell stain kit (Invitrogen, Carlsbad, CA). HIV-1- and/or MV-infected cells were analyzed using flow cytometry (FACSCant II flow cytometer; BD Bioscience, Pharmingen, CA) and a FACSDiva flow cytometer (BD Bioscience) or Flowjo software (Tree Star, San Carlos, CA).

Detection of cytokines. The levels of gamma interferon (IFN-γ), IL-1β, IL-2, IL-5, IL-10, tumor necrosis factor alpha (TNF-α), and TNF-β in the culture supernatant of the HIV-1-infected or mock-infected PBMC cultures were measured using a FlowCytomix human Th1/Th2 11plex kit (Bender MedSystems, Vienna, Austria), according to the manufacturer's protocol, at day 5 postinfection. The minimum detection levels for each cytokine were as follows: IFN-γ, 1.6 pg/ml; IL-1β, 4.2 pg/ml; IL-2, 16.4 pg/ml; IL-4, 20.8 pg/ml; IL-5, 1.6 pg/ml; IL-6, 1.2 pg/ml; IL-8, 0.5 pg/ml; IL-10, 1.9 pg/ml; IL-12 p70, 1.5 pg/ml; TNF-α, 3.2 pg/ml; and TNF-β, 2.4 pg/ml. Results were calculated using FlowCytomix Pro software (Bender MedSystems).

Transwell assay. HIV-1-infected or -uninfected PBMCs were cultured in the top chamber of a transwell plate (pore size, 0.4 μm; Costar; Corning, Corning, NY). HIV-1-uninfected PBMCs were placed on the bottom chamber and cultured for 5 days.

Blocking of antibodies against cell adhesion molecules. An isotype control IgG1 (PeproTech Inc., Rocky Hill, NJ) or serial dilutions of anti-leukocyte function-associated molecule 1α (anti-LFA-1α) or anti-LFA-3 MAbs (serially diluted from 10 μg/ml) were added to HIV-1-infected PBMC cultures just after 2 h of infection to analyze the effect of cell-to-cell contact on SLAM upregulation. Anti-LFA-1α and anti-LFA-3 MAbs were prepared from hybridomas kindly provided by Hideo Yagita (Juntendo University, Tokyo, Japan).

Statistical analysis. Because of the limited sample size, each experiment was performed once per donor. Data obtained from less than three donors were excluded from the statistical analysis. The significance of the data was evaluated by the Mann-Whitney U test, by the Tukey multiple-comparison test, or by use of the Pearson correlation coefficient on the basis of the normality and variance of the data using GraphPad Prism software (version 4.0; GraphPad Software, San Diego, CA). *P* values of <0.05 were considered statistically significant.

RESULTS

HIV-1 infection enhances the infectivity of coinfected MV *ex vivo*. First, the consequences of coinfection of PBMCs with HIV-1 and MV were analyzed at the single-cell level using flow cytometry. DsRed-expressing ($DsRed^+$) HIV-$1_{NL\text{-}D}$- or mock-infected PBMCs were coinfected with GFP-expressing (GFP^+) MVwt or

Downloaded from http://jvi.asm.org/ on January 30, 2013 by National Institute of Infectious Diseases, Murayama Bunshitsu

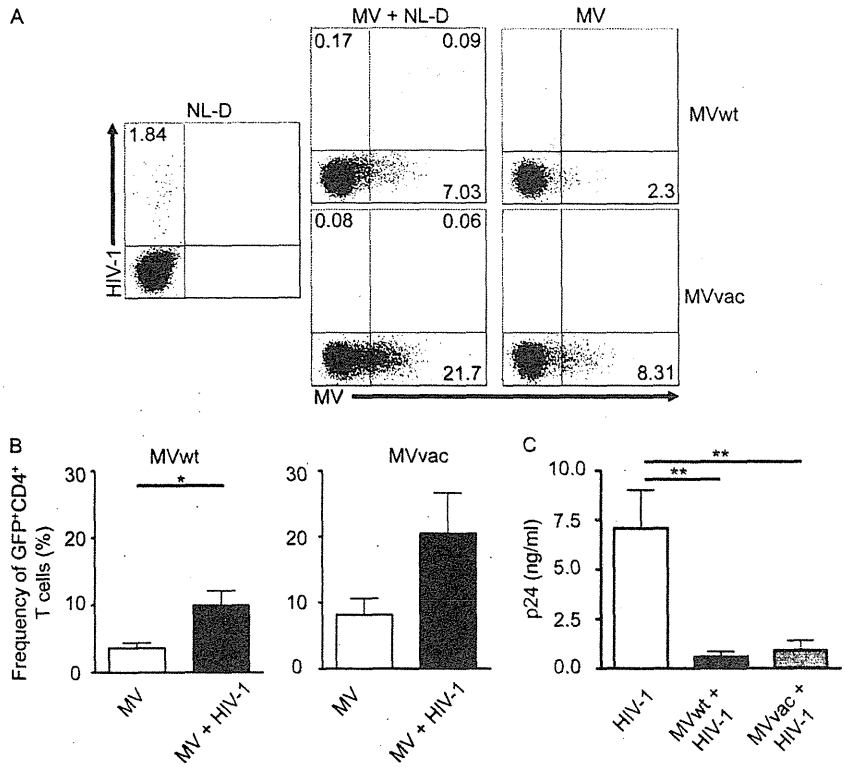

FIG 1 Effect of HIV-1 infection on MV infection in an *ex vivo* HIV-1/MV coinfection model. PBMCs were coinfected with HIV-1_{NL-D} and/or either MVwt or MVvac, and the infected cells were analyzed. (A) Representative flow cytometry plots showing MVwt- or MVvac-infected $CD4^+$ T cells. (B) Cumulative data showing the frequency of MVwt- or MVvac-infected $CD4^+$ T cells. The bars represent the mean ± SEM ($n = 7$). *P* values were calculated using the Mann-Whitney U test. *, $P < 0.05$. (C) Levels of p24 antigen in culture supernatants of HIV-1 and/or MV-infected PBMCs. The bars represent the mean ± SEM ($n = 5$). *P* values were calculated using one-way analysis of variance followed by the Tukey multiple-comparison test. **, $P < 0.01$.

MVvac at day 5. Two days later, HIV- and/or MV-infected cells were analyzed. As shown in Fig. 1A, HIV-1_{NL-D}-infected and MV-infected cells were identified as $DsRed^+$ and GFP^+ cells, respectively. In the case of MVwt infection, the frequency of MVwt-infected $CD4^+$ T cells within the HIV-1_{NL-D}-infected PBMC population (9.96% ± 2.45%) was significantly higher than that in the MV-only-infected PBMC population (3.60% ± 0.77%) ($P = 0.0175$; $n = 7$; Fig. 1B, left). Likewise, in the case of MVvac infection, the frequency of MVvac-infected $CD4^+$ T cells tended to be higher within the HIV-1_{NL-D}-infected PBMC population (20.42% ± 6.20%) than within the MV-only-infected PBMC population (8.14% ± 2.45%), although the result was not statistically significant ($P = 0.1158$; $n = 7$; Fig. 1B, right). These results indicated that HIV-1 infection enhances MV infection in PBMCs. It should be noted that the HIV-infected $CD4^+$ T cell population disappeared upon MV infection (from 1.84% to 0.26% and 0.14% for MVwt and MVvac, respectively), and the doubly infected $CD4^+$ T cell population was rarely visible (Fig. 1A). Although we used the same MOI, the percentage of MV-infected T cells was always higher in MVvac infection than in MVwt infection. This is probably due to the wider tropism of MVvac, which utilizes both SLAM and CD46 as receptors (4).

The level of HIV-1 Gag p24 in the culture supernatant was also significantly reduced by coinfection with either MVwt or MVvac compared with that observed after infection with HIV-1_{NL-D} alone ($P < 0.01$; $n = 5$; Fig. 1C). These results are consistent with those reported previously; i.e., MV infection inhibits the replication of HIV-1 (7, 8, 10).

SLAM expression on $CD4^+$ T cells is induced by HIV-1 infection. Because both MVwt and MVvac utilize SLAM as a receptor (5, 22), SLAM expression was examined in HIV-1-infected PBMCs. PBMCs were infected with either CXCR4-tropic HIV-1_{NL-E}, CCR5-tropic HIV-$1_{NLAD8-E}$, or HIV-1/VSV-G, all of which express GFP, and were then cultured for 5 days without additional stimulation (apart from the addition of IL-2). It is noteworthy that, regardless of HIV-1 infection, SLAM expression was slightly increased under these culture conditions at day 5 (basal increase), and this basal increase varied among individuals (5.17 ± 2.63% at day 0 to 8.81% ± 2.00% at day 5; $n = 7$). Therefore, the net increase in the frequency of $SLAM^{hi}$ $CD4^+$ or $SLAM^{hi}$ $CD8^+$ T cells was calculated by subtracting their respective basal levels of increase. Induction of SLAM expression on $CD8^+$ T cells was low and did not increase statistically significantly with HIV-1 infection (Fig. 2A, bottom, and B, right). However, importantly, both the level of SLAM expression and the frequency of $SLAM^{hi}$ $CD4^+$ T cells increased after infection with HIV-1, and increased SLAM expression was observed in HIV-1-infected (GFP^+) as well as in uninfected $CD4^+$ T cells (Fig. 2A, top). Because the net increase in SLAM expression varied between donors, PBMCs from 10 donors were examined. The frequency of $SLAM^{hi}$ $CD4^+$ T cells markedly increased in the HIV-1_{NL-E}-infected cultures (8.79% ± 1.47%), while the frequency in HIV-1/VSV-G-infected cultures increased only slightly (2.52% ± 0.58%). This difference between HIV-1_{NL-E}- and HIV-1/VSV-G-infected cultures was statistically significant ($P < 0.01$; $n = 10$; Fig. 2B). Of note, HIV-1/VSV-G-infected

Downloaded from http://jvi.asm.org/ on January 30, 2013 by Natinoal Institute of Infectius Diseases, Murayama Bunshitsu

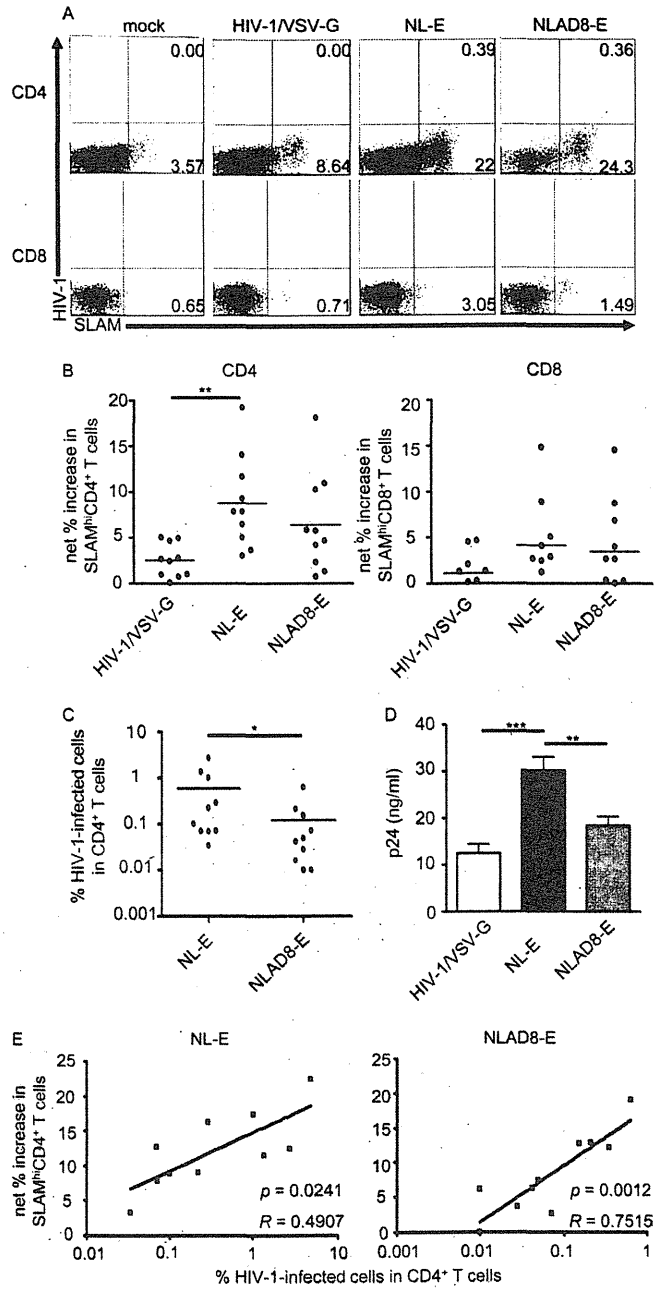

FIG 2 SLAM expression on $CD4^+$ T cells within the HIV-1-infected PBMC population. (A and B) PBMCs were infected with HIV-1/VSV-G, HIV-1_{NL-E}, or HIV-$1_{NLAD8-E}$, and SLAM expression on $CD4^+$ T cells was analyzed. (A) Representative flow cytometry plots showing SLAM expression on $CD4^+$ T cells and $CD8^+$ T cells. (B) Cumulative data showing the percent increase in the frequency of $SLAM^{hi}$ $CD4^+$ and $SLAM^{hi}$ $CD8^+$ T cells from 10 donors. *P* values were calculated using one-way analysis of variance followed by the Tukey multiple-comparison test. **, $P < 0.01$. (C) Cumulative data showing the frequency of HIV-1-infected $CD4^+$ T cells from 10 donors. *P* values were calculated using the Mann-Whitney U test. *, $P < 0.05$. (D) Levels of p24 antigen in culture supernatants of HIV-1-infected PBMCs. The bars represent the mean ± SEM ($n = 10$). *P* values were calculated using one-way analysis of variance followed by the Tukey multiple-comparison test. **, $P < 0.01$; ***, $P < 0.001$. (E) Correlation between the frequency of HIV-1_{NL-E}- and HIV-$1_{NLAD8-E}$-infected $CD4^+$ T cells and the percent increase in the frequency of $SLAM^{hi}$ $CD4^+$ T cells from 10 donors. Correlation statistics were analyzed using the Pearson correlation.

(GFP^+) cells were scarcely detectable under these conditions, probably reflecting the low transduction efficiency of VSV-pseudotyped lentivirus in unstimulated T cells. A marked upregulation of SLAM expression induced by HIV-$1_{NLAD8-E}$ infection was also observed in some donors, but the difference between HIV-$1_{NLAD8-E}$- and HIV-1/VSV-G-infected cultures was not statistically significant (Fig. 2B). This probably reflects the variable number and low frequency of $CCR5^+$ $CD4^+$ T cells (5 to 10% of $CD4^+$ T cells), which are a target of CCR5-tropic HIV-$1_{NLAD8-E}$, in donor PBMCs. As expected, the frequency of HIV-1_{NL-E}-infected $CD4^+$ T cells (0.88% ± 0.28%) was higher than that of HIV-$1_{NLAD8-E}$-infected $CD4^+$ T cells (0.19% ± 0.01%) ($P = 0.0433$; $n = 10$; Fig. 2C). In parallel with the high frequency of $SLAM^{hi}$ $CD4^+$ T cells, the levels of p24 were the highest in the culture supernatants of HIV-1_{NL-E}-infected cultures compared to other HIV-1-infected cultures (Fig. 2D). There was a significant correlation between the frequency of HIV-1-infected $CD4^+$ T cells and that of $SLAM^{hi}$ $CD4^+$ T cells in both HIV-1_{NL-E}-infected ($R = 0.4907$, $P = 0.0241$; $n = 10$) and HIV-$1_{NLAD8-E}$-infected ($R = 0.7517$; $P = 0.0012$; $n = 10$) cultures (Fig. 2E).

To determine whether the replication of HIV-1 was required for SLAM upregulation, PBMCs were infected with a 20-fold higher dose of HIV-1/VSV-G. The frequency of GFP^+ $CD4^+$ T cells and $SLAM^{hi}$ $CD4^+$ T cells under these conditions was identical to that seen in HIV-1_{NL-E}-infected PBMCs (see Fig. S1 in the supplemental material). Taken together, these results indicated that HIV-1 replication is not essential but that higher and/or persistent levels of HIV-1 are involved in the upregulation of SLAM expression on $CD4^+$ T cells.

All subsequent studies were carried out using CXCR4-tropic HIV-1_{NL-E}.

SLAM upregulation by HIV-1 infection is not caused by direct infection of $CD4^+$ T cells. Despite the fact that HIV-1 infection enhanced SLAM expression on $CD4^+$ T cells, upregulation was more obvious in HIV-1-uninfected $CD4^+$ T cells (Fig. 2A). To further test the importance of direct HIV-1 infection of $CD4^+$ T cells for SLAM upregulation, T cells were enriched from PBMCs. PBMCs and T cells were separately infected with HIV-1_{NL-E}, and the expression of SLAM on $CD4^+$ T cells was analyzed after 5 days of culture. A representative result from six individuals is shown in Fig. 3A, and plots from all six individuals are shown, with averages, in Fig. 3B. The majority of HIV-1_{NL-E}-infected $CD4^+$ T cells in the purified T cell cultures were SLAM-dull (Fig. 3A), and the net increase in the frequency of $SLAM^{hi}$ $CD4^+$ T cells (2.87% ± 1.04%) was much lower than that in the PBMC cultures (13.00% ± 3.72%) ($P < 0.01$; $n = 6$; Fig. 3B). To examine in more detail which cell population within the PBMCs contributed to the upregulation of SLAM by HIV-1 infection, whole PBMCs and those depleted of either $CD14^+$ monocytes, $CD19^+$ B cells, or $HLA\text{-}DR^+$ cells were infected with HIV-1_{NL-E}. Cell depletion was evaluated by flow cytometry (Fig. 3C). The removal of $HLA\text{-}DR^+$ cells resulted in depletion of both monocytes and B cells (Fig. 3C, lower right). Of note, a minor population of CD123-, CD141-, and/or CD303-expressing cells (peripheral dendritic cells [pDCs] and conventional dendritic cells [DCs]) were also removed by depletion of $HLA\text{-}DR^+$ cells (data not shown). There were no significant differences in the increase in $SLAM^{hi}$ $CD4^+$ T cells among monocyte- and B cell-depleted PBMCs compared to whole PBMCs following HIV-1 infection in four donors; the relative increases in monocyte- and B cell-depleted PBMCs compared to

Downloaded from http://jvi.asm.org/ on January 30, 2013 by National Institute of Infectious Diseases, Murayama Bunshitsu

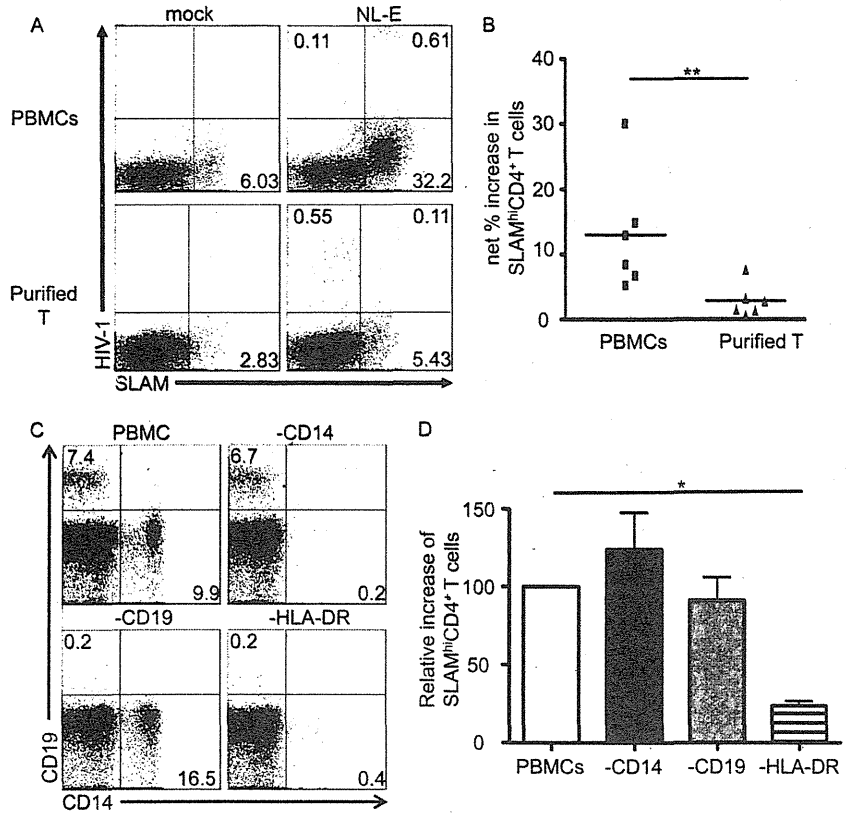

FIG 3 Comparison of the levels of SLAM upregulation on $CD4^+$ T cells induced by HIV-1 infection in the presence or absence of non-T cells. (A and B) Purified T cells and PBMCs were separately infected with HIV-1_{NL-E}. (A) Representative flow cytometry plots showing SLAM expression on $CD4^+$ T cells. (B) Cumulative data showing the percent increase in $SLAM^{hi}$ $CD4^+$ T cells. The bars represent the mean ± SEM ($n = 6$). *P* values were calculated using the Mann-Whitney U test. **, $P < 0.01$. (C and D) PBMCs were infected with HIV-1_{NL-E} after removal of monocytes, B cells, or $HLA\text{-}DR^+$ cells. (C) Representative flow cytometry plot evaluating the depletion of monocytes, B cells, or $HLA\text{-}DR^+$ cells. (D) Cumulative data showing the relative increase in the frequency of $SLAM^{hi}$ $CD4^+$ T cells. The increase in the frequency of $SLAM^{hi}$ $CD4^+$ T cells by HIV-1 infection in the PBMC population was set to 100%. The bars represent the mean ± SEM ($n = 4$). *P* values were calculated using one-way analysis of variance followed by the Tukey multiple-comparison test. *, $P < 0.05$.

whole PBMCs (set at 100%) were 124.1% ± 23.68% and 91.19% ± 14.84%, respectively ($n = 4$). In contrast, SLAM expression was significantly repressed in $HLA\text{-}DR^+$ cell-depleted PBMCs following HIV-1 infection (relative increase, 23.65% ± 3.13%; $n = 4$). Taken together, these results indicated that a population of HLA-DR-expressing cells, including DCs, but not monocytes and B cells, is involved in the upregulation of SLAM by HIV-1 infection.

Role of cytokines in induction of SLAM expression during HIV infection. SLAM expression on T cells and DCs is upregulated by IFN-γ (9) and IL-1β (14), respectively. Therefore, the levels of 11 cytokines (IFN-γ, IL-1β, IL-2, IL-4, IL-5, IL-6, IL-8, IL-10, IL-12 p70, TNF-α, and TNF-β) in the culture supernatants of HIV-1_{NL-E}-infected and -uninfected PBMCs were measured at day 5. The results showed that the production of IFN-γ, IL-1β, and TNF-α in HIV-1_{NL-E}-infected PBMCs was significantly higher than that in uninfected PBMCs ($P = 0.0006$, 0.0023, and 0.0041, respectively; $n = 4$; Fig. 4A). The levels of IL-2, IL-4, IL-5, IL-6, IL-8, IL-10, IL-12 p70, and TNF-β were low or undetectable, irrespective of HIV-1 infection (data not shown). SLAM upregulation on $CD4^+$ T cells was not affected, when HIV-1_{NL-E}-infected PBMCs were cultured in the absence or presence of anti-IFN-γ blocking MAb (data not shown). Furthermore, SLAM upregulation was not observed in PBMC cultures in the presence of recombinant IFN-γ (data not shown).

To test the potential contribution of any soluble factors produced in HIV-1-infected PBMC cultures, we performed a transwell assay. HIV-1_{NL-E}-infected PBMCs were seeded into the top chamber of the transwell, and uninfected PBMCs were placed in the bottom chamber. The cells were then cultured for 5 days. A representative result is shown in Fig. 4B. SLAM was markedly upregulated in HIV-1_{NL-E}-infected PBMCs in the top chamber (net increase, 32.81%; Fig. 4B, upper right), whereas upregulation was less obvious in uninfected PBMCs in the bottom chamber (net increase, 3.35%; Fig. 4B, lower right). The result was reproduced using PBMCs from eight separate donors, and the difference was statistically significant (bottom chamber, 1.07% ± 0.80%; top chamber, 9.08% ± 4.60%; $P < 0.001$; $n = 5$; Fig. 4C). Thus, these data clearly show that soluble factors produced by HIV-1 infection make a minimal contribution (if any) to SLAM upregulation on $CD4^+$ T cells. Rather, cell-to-cell contact would appear to be the most important factor.

Importance of costimulatory molecules for SLAM upregulation on $CD4^+$ T cells. SLAM expression on T cells is induced by T cell receptor (TcR) stimulation with anti-CD3 antibody (3). In addition, Sheng and colleagues showed that LFA-3/CD2 interaction and, particularly, CD2 signaling are necessary but not sufficient for $CD4^+$ T cell activation (25). We showed earlier that in PBMCs, $HLA\text{-}DR^+$ cells are largely responsible for the upregulation of SLAM after HIV-1 infection (Fig. 3C). Previously, we

Downloaded from http://jvi.asm.org/ on January 30, 2013 by National Institute of Infectious Diseases, Murayama Bunshitsu

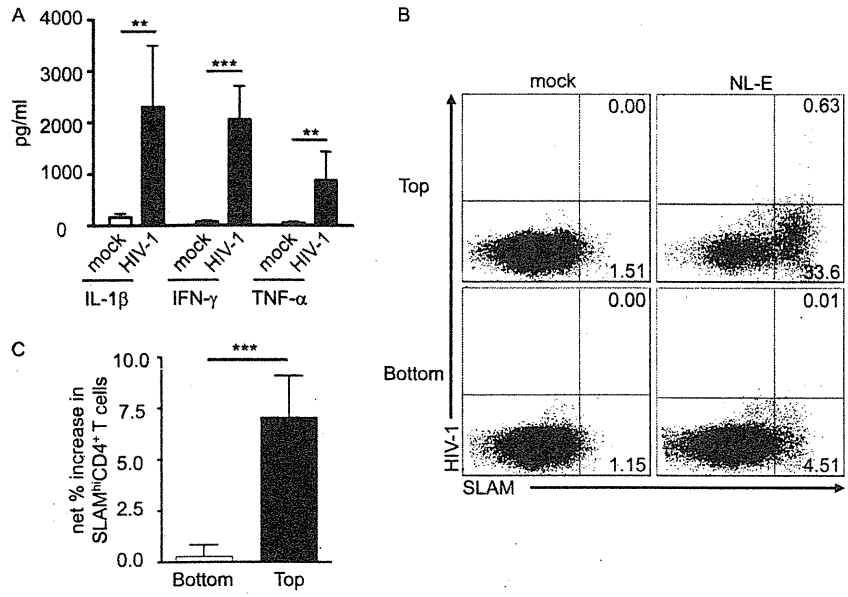

FIG 4 Impact of soluble factors on SLAM upregulation by HIV-1-infected $CD4^+$ T cells. (A) PBMCs were infected with HIV-1_{NL-E}, and the cytokine levels in the culture supernatants were measured. The bars represent the mean ± SEM ($n = 7$). P values were calculated using the Mann-Whitney U test. **, $P < 0.01$; ***, $P < 0.001$. (B and C) HIV-1_{NL-E}- and mock-infected PBMCs were cultured in the top chamber and uninfected PBMCs were placed in the bottom chamber of a transwell plate. (B) Representative flow cytometry plots showing SLAM expression on $CD4^+$ T cells. (C) Percent increase in the frequency of $SLAM^{hi}$ $CD4^+$ T cells. The bars represent the mean ± SEM ($n = 8$). P values were calculated using the Mann-Whitney U test. ***, $P < 0.001$.

showed that HIV-1 replication and expansion are associated with the activation of $CD4^+$ T cells through cell-to-cell contact with monocyte-derived DCs via costimulatory molecules such as LFA-1/intercellular adhesion molecule 1 (ICAM-1) and LFA-3/CD2 (27). We next tested the effect of blocking antibodies that inhibited these interactions on SLAM expression on $CD4^+$ T cells. HIV-1_{NL-E}-infected PBMCs were cultured in the absence or presence of blocking MAbs against LFA-1α and LFA-3. As shown in Fig. 5A, increased SLAM expression on $CD4^+$ T cells within the HIV-1_{NL-E}-infected PBMC population was inhibited by anti-LFA-1α MAb (48.81% ± 18.12%; $n = 5$) as well as by anti-LFA-3 MAb (86.58% ± 6.93%; $n = 5$), although the effect of anti-LFA-1α MAb was less pronounced and was not statistically significant at 10 μg/ml (Fig. 5B). Nevertheless, both anti-LFA-1α and anti-LFA-3 MAbs inhibited SLAM upregulation in a dose-dependent manner (Fig. 5C), and the in-

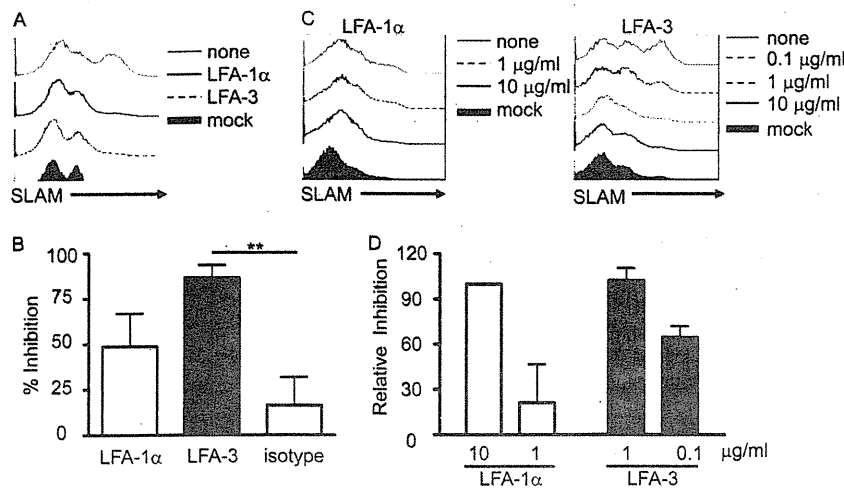

FIG 5 Role of cell-to-cell contact in SLAM upregulation on HIV-1-infected $CD4^+$ T cells. (A and B) HIV-1_{NL-E}-infected PBMCs were cultured in the presence of 10 μg/ml of anti-LFA-1α or anti-LFA-3 MAbs or isotype control IgG1. (A) Representative histogram showing SLAM expression on $CD4^+$ T cells. (B) Percent inhibition of the increase in the frequency of $SLAM^{hi}$ $CD4^+$ T cells. The frequency of $SLAM^{hi}$ $CD4^+$ T cells upregulated by HIV-1 infection was arbitrarily designated 100%. The bars represent the mean ± SEM ($n = 5$). P values were calculated using one-way analysis of variance followed by the Tukey multiple-comparison test. **, $P < 0.01$. (C and D) HIV-1_{NL-E}-infected PBMCs were cultured in the presence of serially diluted concentrations of anti-LFA-1α or anti-LFA-3 MAbs. (C) Representative histogram showing SLAM expression on $CD4^+$ T cells cultured with anti-LFA-1α (left) or anti-LFA-3 (right) MAbs. (D) Relative inhibition of the increase in the frequency of $SLAM^{hi}$ $CD4^+$ T cells. The percent inhibition in the frequency of $SLAM^{hi}$ $CD4^+$ T cells by 10 μg/ml of anti-LFA-1α or anti-LFA-3 MAbs was arbitrarily designated 100%. The bars represent the mean ± SEM ($n = 3$).

Downloaded from http://jvi.asm.org/ on January 30, 2013 by National Institute of Infectious Diseases, Murayama Bunshitsu

hibitory effect of anti-LFA-3 MAb was observed at concentrations as low as 0.1 μg/ml (Fig. 5D).

To confirm whether the inhibition of HIV-1-associated SLAM upregulation by these blocking antibodies also resulted in reduced MV infectivity in $CD4^+$ T cells, HIV-1_{NL-D}-infected PBMCs cultured in the presence of blocking antibodies were infected with MVwt ($n = 2$). As expected, although the frequency of MVwt-infected $CD4^+$ T cells was increased by HIV-1 infection (from 1.30% to 4.51% for donor 1 and from 2.59% to 7.63% for donor 2), the frequency of MVwt-infected cells was reduced by anti-LFA-1α (1.21% and 5.01% for donor 1 and donor 2, respectively) and more strongly by anti-LFA-3 (1.34% and 3.63% for donor 1 and donor 2, respectively) (see Fig. S2 in the supplemental material). These data clearly indicate that SLAM upregulation and the resulting increase in MV-infected $CD4^+$ T cells are mediated by cell-to-cell contact through the interaction of costimulatory molecules that are highly expressed on HLA-DR^+ DC subsets in HIV-1-infected PBMC cultures.

DISCUSSION

The present study shows that HIV-1 infection enhanced MV infection in $CD4^+$ T cells. Interestingly, we observed that the frequencies of MVvac-infected $CD4^+$ T cells were higher than those of MVwt in both HIV-1-infected and -uninfected PBMCs. This difference may be explained by different receptor usage (4) and by differences in polymerase activity between the wild-type and vaccine strains (1) used in this study. In addition, both strains of MV inhibited HIV-1 replication (Fig. 1C), which is consistent with previous reports (7, 8, 10). Although the precise mechanism(s) underlying HIV-1 suppression by MV is not completely understood, the reduction of p24 antigen observed in the culture supernatant occurred in parallel with the elimination of HIV-1-infected cells after MV infection. It is speculated that MV infection causes apoptosis of HIV-1-infected cells directly through the expression of viral nucleoprotein and hemagglutinin proteins (2, 13, 15, 28) or through the induction of cell G_0/G_1 arrest (8), although no doubly infected $CD4^+$ T cells were detected in the culture system used in the present study. Alternatively, considering the fact that HIV-1-infected $CD4^+$ T cells are already activated, they may be hyperactivated by MV, resulting in activation-induced cell death (11).

Because MV utilizes SLAM as a receptor, it is very likely that the enhanced MV infection observed in this *ex vivo* MV and HIV-1 coinfection model was due to HIV-1-induced upregulation of SLAM. Meroni et al. showed that SLAM expression on $CD4^+$ T cells *ex vivo* is diminished during the early phase of HIV infection (16). In addition, SLAM expression on $CD4^+$ T cells was different in patients recently and chronically infected with HIV-1 (16). SLAM expression on $CD4^+$ T cells from HIV-1-infected individuals may fluctuate depending on the activation state of the immune system *in vivo*. It is important to note that most $CD4^+$ T cells within the *ex vivo* PBMC population were in the resting state and that SLAM expression was transiently downregulated soon after the initiation of culture (unpublished observation). SLAM is expressed on activated cells, and chronic hyperactivation is a characteristic feature of HIV-1 infection (11). It was assumed that $CD4^+$ T cells in the PBMC cultures were not hyperactivated and were, rather, akin to the cells within the lymphoid organs, in which a variety of antigen-presenting cells (APCs) and T cells are in contact with each other and where HIV-1 replication/expansion occurs. Therefore, it is possible that SLAM expression is upregulated in lymphoid organs during HIV-1 infection, which may enhance the infectivity of MV.

One of the aims of the present study was to examine the mechanism(s) by which HIV-1 infection enhances SLAM expression on $CD4^+$ T cells. IFN-γ upregulates SLAM expression on T cells in patients with tuberculosis (9, 23). However, neither IFN-γ nor any other soluble factors played a major role in the SLAM upregulation observed in this study. It is possible that SLAM upregulation by IFN-γ is a specific feature of certain T cells reactive to *Mycobacterium tuberculosis*. Nevertheless, the low level of SLAM upregulation induced in T cell culture may be mediated by cytokines, including IFN-γ.

In the present study, blocking experiments showed that cell-to-cell contact (presumably DCs to $CD4^+$ T cells) via LFA-1/ICAM-1 and LFA-3/CD2 interactions enhanced SLAM expression on $CD4^+$ T cells (Fig. 5). Inhibition of the LFA-3/CD2 interaction led to a more marked abrogation of SLAM expression than inhibition of the LFA-1/ICAM-1 interaction. It is noteworthy that a previous study also showed that the LFA-3/CD2 interaction was more important than the LFA-1/ICAM-1 interaction for antigen-dependent DC-T cell synapse formation (27). Therefore, CD2 costimulatory signals, in addition to TcR signals, may be involved in SLAM upregulation. Potential candidate APCs that interact with $CD4^+$ T cells to upregulate SLAM on $CD4^+$ T cells in HIV-infected PBMC cultures could be HLA-DR^+ DCs.

In conclusion, the precise mechanism(s) by which MV exacerbates the disease outcomes in HIV-1-infected individuals remains unknown. The present study, which employed a PBMC-based *ex vivo* HIV-1 and MV coinfection model, showed that increased susceptibility to MV infection involves induction of a high level of SLAM expression by HIV-1 infection via cell-to-cell contact. This is the first report showing a direct relationship between HIV-1 infection and SLAM expression. The high mortality and morbidity of measles in children coinfected with HIV-1 and MV may be due to upregulation of SLAM expression on $CD4^+$ T cells, which presumably occurs within lymphoid organs through T cell contact with DCs during HIV-1 infection. Further *in vivo* coinfection studies in a macaque model should help to clarify these outstanding issues.

ACKNOWLEDGMENTS

We thank Kahori Okano for her excellent technical assistance.

This work was supported by a grant from the Ministry of Health, Labor, and Welfare of Japan. Y.-Y. Mitsuki receives support from the Japanese Foundation for AIDS Prevention.

REFERENCES

1. Bankamp B, Kearney SP, Liu X, Bellini WJ, Rota PA. 2002. Activity of polymerase proteins of vaccine and wild-type measles virus strains in a minigenome replication assay. J. Virol. 76:7073–7081.
2. Bhaskar A, Bala J, Varshney A, Yadava P. 2011 Expression of measles virus nucleoprotein induces apoptosis and modulates diverse functional proteins in cultured mammalian cells. PLoS One 6:e18765. doi:10.1371/journal.pone.0018765.
3. Cocks BG, et al. 1995. A novel receptor involved in T-cell activation. Nature 376:260–263.
4. Condack C, Grivel JC, Devaux P, Margolis L, Cattaneo R. 2007. Measles virus vaccine attenuation: suboptimal infection of lymphatic tissue and tropism alteration. J. Infect. Dis. 196:541–549.
5. Erlenhoefer C, et al. 2001. CD150 (SLAM) is a receptor for measles virus but is not involved in viral contact-mediated proliferation inhibition. J. Virol. 75:4499–4505.

Downloaded from http://jvi.asm.org/ on January 30, 2013 by National Institute of Infectious Diseases, Murayama Bunshitsu

6. **Fujino M, et al.** 2007. Development of a new neutralization test for measles virus. J. Virol. Methods **142**:15–20.
7. **Garcia M, Yu XF, Griffin DE, Moss WJ.** 2005. In vitro suppression of human immunodeficiency virus type 1 replication by measles virus. J. Virol. 79:9197–9205.
8. **Garcia M, Yu XF, Griffin DE, Moss WJ.** 2008. Measles virus inhibits human immunodeficiency virus type 1 reverse transcription and replication by blocking cell-cycle progression of CD4+ T lymphocytes. J. Gen. Virol. 89:984–993.
9. **Garcia VE, et al.** 2001. Signaling lymphocytic activation molecule expression and regulation in human intracellular infection correlate with Th1 cytokine patterns. J. Immunol. 167:5719–5724.
10. **Grivel JC, Garcia M, Moss WJ, Margolis LB.** 2005. Inhibition of HIV-1 replication in human lymphoid tissues ex vivo by measles virus. J. Infect. Dis. 192:71–78.
11. **Haas A, Zimmermann K, Oxenius A.** 2011. Antigen-dependent and -independent mechanisms of T and B cell hyperactivation during chronic HIV-1 infection. J. Virol. 85:12102–12113.
12. **Hashimoto K, et al.** 2002. SLAM (CD150)-independent measles virus entry as revealed by recombinant virus expressing green fluorescent protein. J. Virol. 76:6743–6749.
13. **Iwasa T, Suga S, Qi L, Komada Y.** 2010. Apoptosis of human peripheral blood mononuclear cells by wild-type measles virus infection is induced by interaction of hemagglutinin protein and cellular receptor, SLAM via caspase-dependent pathway. Microbiol. Immunol. 54:405–416.
14. **Kruse M, et al.** 2001. Signaling lymphocytic activation molecule is expressed on mature CD83+ dendritic cells and is up-regulated by IL-1 beta. J. Immunol. 167:1989–1995.
15. **Laine D, et al.** 2005. Measles virus nucleoprotein induces cell-proliferation arrest and apoptosis through NTAIL-NR and NCORE-FcgammaRIIB1 interactions, respectively. J. Gen. Virol. 86:1771–1784.
16. **Meroni L, et al.** 1999. Altered signaling lymphocytic activation molecule (SLAM) expression in HIV infection and redirection of HIV-specific responses via SLAM triggering. Clin. Immunol. 92:276–284.
17. **Moss WJ, Cutts F, Griffin DE.** 1999. Implications of the human immunodeficiency virus epidemic for control and eradication of measles. Clin. Infect. Dis. 29:106–112.
18. **Moss WJ, et al.** 2008. HIV type 1 infection is a risk factor for mortality in hospitalized Zambian children with measles. Clin. Infect. Dis. **46**: 523–527.
19. **Moss WJ, et al.** 2007. Immunogenicity of standard-titer measles vaccine in HIV-1-infected and uninfected Zambian children: an observational study. J. Infect. Dis. 196:347–355.
20. **Muhlebach MD, et al.** 2011. Adherens junction protein nectin-4 is the epithelial receptor for measles virus. Nature **480**:530–533.
21. **Noyce RS, et al.** 2011. Tumor cell marker PVRL4 (nectin 4) is an epithelial cell receptor for measles virus. PLoS Pathog. 7:e1002240. doi:10.1371/journal.ppat.1002240.
22. **Ono N, et al.** 2001. Measles viruses on throat swabs from measles patients use signaling lymphocytic activation molecule (CDw150) but not CD46 as a cellular receptor. J. Virol. 75:4399–4401.
23. **Pasquinelli V, et al.** 2004. Expression of signaling lymphocytic activation molecule-associated protein interrupts IFN-gamma production in human tuberculosis. J. Immunol. 172:1177–1185.
24. **Permar SR, et al.** 2007. Clinical measles after measles virus challenge in simian immunodeficiency virus-infected measles virus-vaccinated rhesus monkeys.. J. Infect. Dis. 196:1784–1793.
25. **Shen A, et al.** 2007. Novel pathway for induction of latent virus from resting $CD4^+$ T cells in the simian immunodeficiency virus/macaque model of human immunodeficiency virus type 1 latency.. J. Virol. **81**: 1660–1670.
26. **Takeda M, et al.** 2006. Generation of measles virus with a segmented RNA genome. J. Virol. **80**:4242–4248.
27. **Tsunetsugu-Yokota Y, et al.** 1997. Efficient virus transmission from dendritic cells to CD4+ T cells in response to antigen depends on close contact through adhesion molecules. Virology 239:259–268.
28. **Vuorinen T, Peri P, Vainionpaa R.** 2003. Measles virus induces apoptosis in uninfected bystander T cells and leads to granzyme B and caspase activation in peripheral blood mononuclear cell cultures. Eur. J. Clin. Invest. 33:434–442.
29. **Yamamoto T, et al.** 2009. Selective transmission of R5 HIV-1 over X4 HIV-1 at the dendritic cell-T cell infectious synapse is determined by the T cell activation state. PLoS Pathog. 5:e1000279. doi:10.1371/journal.ppat.1000279.

Downloaded from http://jvi.asm.org/ on January 30, 2013 by National Institute of Infectious Diseases, Murayama Bunshitsu

Journal of Virology

The SI Strain of Measles Virus Derived from a Patient with Subacute Sclerosing Panencephalitis Possesses Typical Genome Alterations and Unique Amino Acid Changes That Modulate Receptor Specificity and Reduce Membrane Fusion Activity

Fumio Seki, Kentaro Yamada, Yuichiro Nakatsu, Koji Okamura, Yusuke Yanagi, Tetsuo Nakayama, Katsuhiro Komase and Makoto Takeda

***J. Virol.* 2011, 85(22):11871. DOI: 10.1128/JVI.05067-11.**
Published Ahead of Print 14 September 2011.

Updated information and services can be found at:
http://jvi.asm.org/content/85/22/11871

These include:

SUPPLEMENTAL MATERIAL Supplemental material

REFERENCES This article cites 69 articles, 28 of which can be accessed free at: http://jvi.asm.org/content/85/22/11871#ref-list-1

CONTENT ALERTS Receive: RSS Feeds, eTOCs, free email alerts (when new articles cite this article), more»

Information about commercial reprint orders: **http://journals.asm.org/site/misc/reprints.xhtml**
To subscribe to to another ASM Journal go to: **http://journals.asm.org/site/subscriptions/**

Journals.ASM.org

Downloaded from http://jvi.asm.org/ on January 30, 2013 by NATL INST OF INFECTIOUS DISEAS

JOURNAL OF VIROLOGY, Nov. 2011, p. 11871–11882 Vol. 85, No. 22
0022-538X/11/$12.00 doi:10.1128/JVI.05067-11
Copyright © 2011, American Society for Microbiology. All Rights Reserved.

The SI Strain of Measles Virus Derived from a Patient with Subacute Sclerosing Panencephalitis Possesses Typical Genome Alterations and Unique Amino Acid Changes That Modulate Receptor Specificity and Reduce Membrane Fusion Activity▽‡

Fumio Seki,[1]* Kentaro Yamada,[1]† Yuichiro Nakatsu,[1] Koji Okamura,[2] Yusuke Yanagi,[2] Tetsuo Nakayama,[3] Katsuhiro Komase,[1] and Makoto Takeda[1]

Department of Virology 3, National Institute of Infectious Diseases, Tokyo,[1] Department of Virology, Faculty of Medicine, Kyushu University, Fukuoka,[2] and Laboratory of Viral Infection I, Kitasato Institute for Life Sciences, Kitasato University, Tokyo,[3] Japan

Received 10 May 2011/Accepted 31 August 2011

Subacute sclerosing panencephalitis (SSPE) is a fatal sequela associated with measles and is caused by persistent infection of the brain with measles virus (MV). The SI strain was isolated in 1976 from a patient with SSPE and shows neurovirulence in animals. Genome nucleotide sequence analyses showed that the SI strain genome possesses typical genome alterations for SSPE-derived strains, namely, accumulated amino acid substitutions in the M protein and cytoplasmic tail truncation of the F protein. Through the establishment of an efficient reverse genetics system, a recombinant SI strain expressing a green fluorescent protein (rSI-AcGFP) was generated. The infection of various cell types with rSI-AcGFP was evaluated by fluorescence microscopy. rSI-AcGFP exhibited limited syncytium-forming activity and spread poorly in cells. Analyses using a recombinant MV possessing a chimeric genome between those of the SI strain and a wild-type MV strain indicated that the membrane-associated protein genes (M, F, and H) were responsible for the altered growth phenotype of the SI strain. Functional analyses of viral glycoproteins showed that the F protein of the SI strain exhibited reduced fusion activity because of an E300G substitution and that the H protein of the SI strain used CD46 efficiently but used the original MV receptors on immune and epithelial cells poorly because of L482F, S546G, and F555L substitutions. The data obtained in the present study provide a new platform for analyses of SSPE-derived strains as well as a clear example of an SSPE-derived strain that exhibits altered receptor specificity and limited fusion activity.

Measles is an acute highly contagious disease characterized by high fever and a maculopapular rash. Acute measles is accompanied by temporary and severe immunosuppression, and pneumonia caused by secondary bacterial infections is a major cause of measles-related death in children. Subacute sclerosing panencephalitis (SSPE) is a fatal sequela associated with measles. It occurs at a mean latency period of 7 to 10 years after the acute measles stage of development (3, 52). SSPE is caused by persistent infection of the central nervous system (CNS) with measles virus (MV), and suffering from acute measles at an early age is a risk factor for developing SSPE (17). A recent analysis indicated that the risk of developing SSPE was 22 cases per 100,000 reported cases of acute measles (3).

The causative agent, MV, is an enveloped virus that belongs to the genus *Morbillivirus* in the family *Paramyxoviridae*. MV possesses a nonsegmented, negative-sense RNA genome that includes six linked tandem genes, N, P/V/C, M, F, H, and L. The genome is encapsidated by the nucleocapsid (N) protein and is associated with a viral RNA-dependent RNA polymerase composed of phosphoproteins (P proteins) and large proteins (L proteins) that form a ribonucleoprotein (RNP) complex (12). Two types of glycoprotein spikes, the hemagglutinin (H) and fusion (F) proteins, are expressed on the viral envelope. The H protein is responsible for binding to cellular receptors on the target host cells. The signaling lymphocyte activation molecule (SLAM) expressed on immune system cells functions as the principal receptor for MV (62, 69). We and another group recently demonstrated that certain epithelial cells that form tight junctions express an unidentified receptor for MV that is designated the epithelial cell receptor (ECR) (25, 50, 59). Binding of the H protein to a receptor triggers F protein-mediated membrane fusion of the virus envelope and the host cell plasma membrane (12). These proteins are also expressed on the cell surface and cause cell-to-cell fusion. The matrix (M) protein plays crucial roles in the process of virus assembly via its interaction with both the RNP and the cytoplasmic tails of the glycoproteins. MV strains derived from patients with SSPE (SSPE strains) generally do not express a functional M protein, becoming defective in producing infectious virus particles, and thus spread via cell-to-cell fusion (10, 14–16, 18). In addition, SSPE strains usually have a deletion or an alteration in the cytoplasmic tail of the F protein (4, 9, 31, 44).

* Corresponding author. Mailing address: Department of Virology 3, National Institute of Infectious Diseases, Gakuen 4-7-1, Musashimurayama 208-0011, Tokyo, Japan. Phone: 81-42-561-0771. Fax: 81-42-562-8941. E-mail: fseki@nih.go.jp.

† Present address: Research Promotion Project, Oita University, Oita, Japan.

‡ Supplemental material for this article may be found at http://jvi.asm.org/.

▽ Published ahead of print on 14 September 2011.

Downloaded from http://jvi.asm.org/ on January 30, 2013 by NATL INST OF INFECTIOUS DISEAS

The SI strain was isolated in 1976 from a patient with SSPE by cultivating brain tissue biopsy samples with Vero cells (29). The patient was 8 years of age and had suffered from acute measles at 4 years of age (29). The SI strain was found to show neurovirulence, and all animals (mice, hamsters, and guinea pigs) inoculated intracerebrally with the SI strain showed neurological manifestations at 3 to 6 days after inoculation and eventually died (29). Despite these significant characteristics, molecular analyses of the SI strain have been poorly conducted. In the present study, we identified unique characteristics of the SI strain and identified substitutions responsible for the modulated receptor specificity and reduced membrane fusion activity. The present study also obtained data using a genetic engineering system of the SI strain expressing a fluorescent protein. This system could be a new platform for analyses of the molecular bases and pathogenesis of SSPE.

MATERIALS AND METHODS

Cells. BHK/T7-9 cells constitutively expressing T7 RNA polymerase (20) were maintained in Dulbecco's minimum essential medium (DMEM; Sigma, St. Louis, MO) supplemented with 7% fetal bovine serum (FBS). Vero/hSLAM (36) and CV1/hSLAM (58), which constitutively express human SLAM (hSLAM), were maintained in DMEM supplemented with 7% FBS and 0.5 mg/ml Geneticin (G418; Invitrogen Life Technologies, Carlsbad, CA). CHO cells and A549 cells constitutively expressing human SLAM, CHO/hSLAM (62), and A549/hSLAM (57), respectively, were maintained in RPMI medium (Invitrogen) supplemented with 7% FBS and 0.5 mg/ml G418. Vero cells and IMR-32 cells were maintained in DMEM supplemented with 7% FBS and 10% FBS, respectively. H358 (59) and II-18 (49) cells were maintained in RPMI supplemented with 10% FBS. SH-SY5Y cells were maintained in DMEM/F12 (Invitrogen) supplemented with 10% FBS (49, 59).

Plasmid constructions. The first-strand cDNA of the SI strain antigenome was synthesized by reverse transcription of total RNA isolated from Vero/hSLAM cells infected with the SI strain. Eight DNA fragments covering the entire region of the SI strain genome were then generated by PCR. These fragments were cloned into pBluescriptII KS(+) vector (Agilent Technologies, Inc., Santa Clara, CA) in a stepwise manner, generating a plasmid carrying the full-length antigenomic cDNA of the SI strain (detailed procedure provided upon request). A hammerhead ribozyme sequence (HHRz) was added between the T7 promoter sequence and the MV genome cDNA by a combination of PCR procedures using the synthesized DNA (5′-**GTGAATTGTAATACGACTCACTATAGGG***TGTTTG GTCTGATGAGGCCGAAAGGCCGAAACTCCGTAAGGAGTC*ACCAAACA AA-3′; the T7 promoter and HHRz sequences are shown in boldface and italics, respectively, and the MV genome cDNA sequence is underlined). To generate an additional transcriptional unit for a green fluorescent protein (GFP) derived from *Aequorea coerulescens* (AcGFP; Clontech, Palo Alto, CA), a fragment containing the open reading frame (ORF) of AcGFP was amplified by PCR using primer pair 5′-*GGCGCGCC***ATG**GTGAGCAAG-3′ and 5′-*GACGTC***TT** ACTTGTACAGCTCGT-3′ (sequences corresponding to the AscI and AatII sites are shown in italics; sequences corresponding to the initiation and termination codons are shown in boldface). The fragment was combined with the synthesized cDNA fragments containing the region between the H and L protein open reading frames of the IC-B strain by a combination of PCR procedures. The nucleotide sequences of the synthesized cDNA fragments were 5′-**ACTAGT**GAAATAGACA TCAGAATTAAGAAAAACGTAGGGTCCAAGTGGTTTCCCGTT*GGCGCG CC*-3′ and 5′-*GACGTC*TGCCAGTGAACCGATCACATGATGTCACCCAGAC ATCAGGCATACCC**ACTAGT**-3′ (sequences corresponding to SpeI sites are shown in boldface, sequences corresponding to AscI and AatII sites are shown in italics, and sequences corresponding to the gene end [GE] of the H gene and gene start [GS] of the L gene are underlined). The fragment containing the transcriptional unit for AcGFP was then inserted into the SpeI site between the H and L genes. The generated construct was named pHHRz-SI-AcGFP. Using a similar procedure, the additional transcriptional unit for AcGFP was also inserted into the p(+)MV323 plasmid, which carries the full-length antigenomic cDNA of the IC-B strain (60). The resulting plasmid was named p(+)MV323-AcGFP. A SalI-AatII fragment containing a region of the M, F, and H genes of p(+)MV323-AcGFP was replaced with a corresponding fragment of pHHRz-SI-AcGFP, and the generated construct was named p(+)MV323/SI-MFH-AcGFP. A SalI-BstEII fragment containing a region of the M gene of the pHHRz-SI-AcGFP was replaced with a corresponding fragment of p(+)MV323, and the generated construct was named pHHRz-SI/ICM-AcGFP. To generate support plasmids for the rescue of recombinant MVs from cloned cDNAs, DNA fragments encoding the N, P, and L proteins of the wild-type (wt) MV strains (IC-B or 9301B) were cloned into the pCITE vector (Novagen, Madison, WI), generating pCITE-IC-N, pCITE-IC-PΔC, and pCITEko-9301B-L, respectively. DNA fragments encoding the M proteins of the IC-B and SI strains fused with a red fluorescent protein, mCherry (Clontech), at the carboxyl-terminal end were generated by a combination of PCR procedures and inserted into a mammalian expression vector, pCA7 (32, 57). The resulting plasmids were named pCA7-FR-IC-M-mCherry and pCA7-FR-SI-mCherry, respectively. DNA fragments encoding the F proteins of the IC-B and SI strains were also amplified by PCR and cloned into pCAGGS (32), generating pCAGGS-IC-F and pCAGGS-SI-F, respectively. Similarly, DNA fragments encoding the H proteins of the IC-B and SI strains were amplified and cloned into pCAGGS, generating pCAGGS-IC-H and pCAGGS-SI-H, respectively. By replacing the SalI-XhoI, EcoRI-SalI, KpnI-XhoI, and SalI-KpnI regions of pCAGGS-IC-F with the corresponding region of pCAGGS-SI-F, four plasmids encoding chimeric F proteins between the IC-B and SI strains, designated pCAGGS-IC/SI-F-1, -F-2, -F-3, and -F-4, respectively, were generated. An amino acid substitution, G300E, was introduced into pCAGGS-SI-F, and five other amino acid substitutions, N390M, L482F, S546G, F555L, and I564L, were introduced independently into pCAGGS-IC-H by site-directed mutagenesis using complementary primer pairs.

Antibodies. A mouse monoclonal antibody (MAb) against CD46 (M75) was kindly provided by T. Seya (46). Mouse MAbs against the proteins encoded by MV H (B5), F (C527), and M (A23, A24, A27, A154, A157, A177, B46, A39, A41, A42, A51, and A133) were kindly provided by T. A. Sato (42).

Viruses. BHK/T7-9 cells were transfected with full-length genome plasmids carrying the antigenomes of MV and three support plasmids, pCITE-IC-N, pCITE-IC-PΔC, and pCITEko-9301B-L, by the use of Lipofectamine LTX Plus reagent (Invitrogen). After 2 days, the transfected cells were cocultured with Vero/hSLAM cells. IC323-AcGFP, SI-AcGFP, IC/SI-MFH-AcGFP, and SI/ICM-AcGFP were generated from p(+)MV323-AcGFP, pHHRz-SI-AcGFP, p(+)MV323/SI-MFH-AcGFP, and pHHRz-SI/ICM-AcGFP, respectively. The generated MVs were propagated in Vero/hSLAM cells. Infectious virus-like particles of SI-AcGFP and IC/SI-MFH-AcGFP were prepared by incubating the cells with 5 μg/ml cytochalasin D (Sigma) at 35°C for 30 min, as described previously (19). The infectious virus-like particles were concentrated using PEG-it precipitation solution (System Biosciences Inc., Mountain View, CA). The cell infectious units (CIUs) of the recombinant MVs expressing a fluorescent protein were determined using Vero/hSLAM cells, as described previously (51). To analyze the cytopathic effects (CPEs), monolayers of cells in 6-well cluster plates were infected with 500 CIUs of MV and the cells were observed daily using an Axio Observer.D1 microscope (Carl Zeiss, Jena, Germany).

Virus growth. Monolayers of Vero/hSLAM cells in 24-well plates were infected with recombinant MVs at a multiplicity of infection (MOI) of 0.01 per cell. At various time intervals, cell-free virus was obtained from the culture supernatants, and cell-associated virus was recovered from infected cells in 0.5 ml of DMEM-supplemented 7% FBS by freezing and thawing.

Virus titration. Monolayers of Vero/hSLAM cells in 6-well cluster plates were infected with serially diluted virus samples, incubated for 1 h at 37°C, and overlaid with DMEM containing 7% FBS and 1% agarose. PFU numbers were determined by counting the number of plaques.

Phylogenic tree analysis and Ka/K_s calculation. Nucleotide and amino acid sequence alignments and a phylogenic distance analysis were performed with the ClustalW program (63) at the genomeNet website maintained by the Kyoto University Bioinformatics Center. A phylogenic tree constructed using SI, IC-B, 9301B, WA.USA/17.98, and reference strains (66) was drawn using FigTree software. Ka/K_s calculations were performed using KaKs Calculator version 2.0 software (64). Briefly, using the two nucleotide sequences of each protein-coding region, the nonsynonymous and synonymous substitution rates (Ka and K_s, respectively) were calculated by counting the numbers of nonsynonymous and synonymous sites (NA and NS, respectively) and the numbers of nonsynonymous and synonymous substitutions (MA and MS, respectively). MA/NA and MS/NS represent the Ka and K_s substitution rates, respectively.

Immunofluorescence staining. Monolayers of Vero/hSLAM cells were seeded in 24-well plates or on coverslips in six-well cluster plates. Some monolayers were transfected with expression plasmids encoding M protein tagged with mCherry or not tagged. Other monolayers were infected with recombinant MVs and incubated with 50 μg/ml of a fusion-blocking peptide, Z-D-Phe-Phe-Gly (Peptide Institute Inc., Osaka, Japan), as described previously (41). At 24 h posttransfection or at 2 or 5 days postinoculation (p.i.) (using IC323-AcGFP or SI-AcGFP,

Downloaded from http://jvi.asm.org/ on January 30, 2013 by NATL INST OF INFECTIOUS DISEAS

respectively), the cells were fixed and permeabilized with phosphate-buffered saline containing 2.5% formaldehyde and 0.5% Triton X-100. The cells were then stained with a mouse MAb against the M protein for 1 h at room temperature, followed by incubation with an Alexa Fluor 488- or 594-conjugated secondary antibody (Molecular Probes, Eugene, OR) for 1 h at room temperature. The nuclei of the infected cells were stained with 4′,6′-diamidino-2-phenylindole (DAPI; Nacalai Tesque, Kyoto, Japan) at 0.2 μg/ml. The cells were observed using a FluoView FV1000 confocal microscope (Olympus, Tokyo, Japan).

Cell-to-cell fusion assay. CHO/hSLAM, CV1/hSLAM, Vero, H358, or II-18 cells were seeded in 24-well plates, transfected with the H protein-expressing plasmid (0.5 μg) together with the F protein-expressing plasmid (0.5 μg), and incubated in the presence or absence of an anti-CD46 antibody (M75). At 1, 2, or 3 days posttransfection, the cells were fixed with methanol and stained with Giemsa solution (Sigma). The stained cells were observed under an Axio Observer.D1 microscope. To quantify cell-to-cell fusion, monolayers of cells were transfected with H protein-expressing plasmid (0.3 μg) and F protein-expressing plasmid (0.3 μg) together with a red fluorescent protein (mCherry)-expressing plasmid (0.3 μg). At 48 h posttransfection, areas expressing mCherry autofluorescence were measured using an Axio Observer.D1 microscope and ImageJ software (http://rsbweb.nih.gov/ij/index.html). Statistical analyses were performed using Microsoft Excel version 14.1.2 software.

Flow cytometry. CHO/hSLAM cells were transfected with the H or F protein-expressing plasmid (0.5 μg). At 24 h posttransfection, the cells were incubated with mouse MAbs B5 and C527 specific for the H and F proteins, respectively, followed by incubation with an Alexa Fluor 488-conjugated goat anti-mouse secondary antibody (Molecular Probes). The cells were analyzed using a FACSCalibur flow cytometer (Becton Dickinson, Franklin Lakes, NJ).

Minigenome assay. BHK/T7-9 cells were transfected with 0.2 μg of p18MGFLuc01 minigenome plasmid (23) together with 0.2 μg of pCITE-IC-N and various amounts of pCITE-IC-PΔC and pCITEko-9301B-L. At 48 h posttransfection, the enzymatic activity of firefly luciferase was measured using a Dual Glo luciferase assay system (Promega, Madison, WI) and a Mithras LB 940 luminometer (Berthold Technologies, Bad Wildbad, Germany).

Nucleotide sequence accession number. The nucleotide sequence of the SI strain is available under GenBank accession number JF791787.

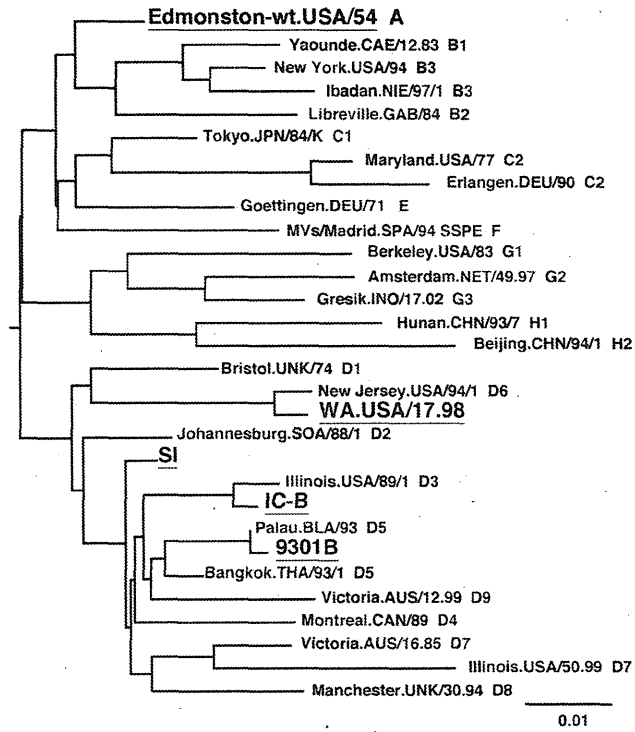

FIG. 1. Phylogenic tree drawn on the basis of the 450-nucleotide sequence that encodes the carboxyl-terminal 150 amino acids of the N protein. The names of the strains used for sequence comparisons in this study (Edmonston-wt, SI, IC-B, 9301B, and WA.USA/17.98) are underlined.

RESULTS

Characterization of the genome of the SI strain. We determined the entire genome nucleotide sequence of the SI strain. A phylogenic tree drawn on the basis of the 450-nucleotide sequence that encodes the carboxyl-terminal 150 amino acids of the N protein showed that the SI strain was classified into clade D but did not belong to a specific genotype (Fig. 1). Genotype analyses performed using a program at a website for measles nucleotide surveillance (MeaNS) (http://www.hpa-bioinformatics.org.uk/Measles/Public/Web_Front/main.php) confirmed the data for the phylogenic tree analysis (see Table S1 in the supplemental material). The entire genome nucleotide sequence of the SI strain was compared with those of three other strains in clade D, strain IC-B (genotype D3; GenBank accession number NC_001498), strain 9301B (genotype D5; GenBank accession number AB012948), and strain WA.USA/17.98 (genotype D6; GenBank accession number DQ227321) (2, 54, 61). The nucleotide sequences of the regulatory regions (i.e., the gene start, gene end, and intergenic sequences) (38) were highly conserved in the SI strain genome. As indicated in previous reports (9, 11, 68), highly biased uracil-to-cystine substitutions were observed in the M gene (see Table S2 in the supplemental material). As also observed for other SSPE strains, nonsynonymous substitutions were accumulated in the M protein reading frame of the SI strain (see Fig. S1 in the supplemental material). The data for the comparison between the SI and IC-B strains are shown in the present paper, but similar results were obtained in the comparisons between the SI and other clade D MV strains. The Ka/K_s ratios were analyzed to reveal differences between the SI and clade D MV strains (IC/SI, 9301/SI, and WA98/SI) and between the Edmonston wild-type (wt) strain (genotype A; GenBank accession number AF266288) and clade D MV strains (IC/Edwt, 9301/Edwt, and WA98/Edwt) (37) (the phylogenic tree in Fig. 1 shows the relationships among the SI, IC-B, 9301B, WA.USA/17.98, and Edmonston wt strains). The data of comparisons between the Edmonston wt and clade D MV strains mostly reflect the selection pressure that operated during the natural evolution of wt MVs, while the data showing comparisons between the SI and clade D MV strains reflect the selection pressure that operated during persistent infection in the brain in addition to the natural evolution of MV. Previously, a similar study was performed by Woelk et al. (67). For the M protein reading frame, the Ka/K_s ratios in the comparisons between the Edmonston wt and clade D MV strains were ~0.03, whereas the ratios in the comparisons between the SI and clade D MV strains were 11 to 12 times greater than those observed in comparisons between the Edmonston wt and clade D MV strains (Table 1), confirming that a dynamic selection or a reduced stabilizing selection pressure operated for the M protein of the SI strain, as observed for other SSPE strains (67). Similarly, although the amino acid sequence of the F protein was highly conserved during the natural evolution of MV (Ka/K_s = 0.0000 ~ 0.0359), this was not the case during persistent infection in the brain (Ka/K_s = 0.1825 ~ 0.2504) (Table 1). Compared with those of IC-B, 12 amino acid changes were found in the F protein of the SI strain, including

Downloaded from http://jvi.asm.org/ on January 30, 2013 by NATL INST OF INFECTIOUS DISEAS

TABLE 1. K_s, Ka, and Ka/K_s values from comparisons of Edmonston wild-type, IC-B, 9301B, WA.USA/17.98, and SI strains[a]

Protein reading frame	Gene region(s)	Nucleotides[b]	K_s		Ka		Ka/K_s	
			IC(D3)/Edwt, 9301(D5)/Edwt, WA98(D6)/Edwt	IC(D3)/SI, 9301(D5)/SI, WA98(D6)/SI	IC(D3)/Edwt, 9301(D5)/Edwt, WA98(D6)/Edwt	IC(D3)/SI, 9301(D5)/SI, WA98(D6)/SI	IC(D3)/Edwt, 9301(D5)/Edwt, WA98(D6)/Edwt	IC(D3)/SI, 9301(D5)/SI, WA98(D6)/SI
N		1–1578	0.0790, 0.0960, 0.1033	0.0512, 0.0703, 0.1218	0.0117, 0.0113, 0.0092	0.0046, 0.0050, 0.0075	0.1486, 0.1178, 0.0892	0.0898, 0.0712, 0.0618
P	P	1–1524	0.0416, 0.0443, 0.0330	0.0246, 0.0273, 0.0330	0.0114, 0.0176, 0.0132	0.0079, 0.0141, 0.0096	0.2740, 0.3981, 0.3982	0.3195, 0.5150, 0.2918
	P/C	22–582	0.0222, 0.0223, 0.0297	0.0073, 0.0074, 0.0147	0.0191, 0.0239, 0.0215	0.0024, 0.0071, 0.0047	0.8596, 1.0739, 0.7241	0.3217, 0.9645, 0.3212
	P/V	691–903	0.0178, 0.0177, 0	0.0177, 0.0176, 0	0, 0.0064, 0.0129	0.0195, 0.0262, 0.0327	0, 0.3643, NA[c]	1.0991, 1.4842, NA
	P′	1–21 + 583–690 + 904–1524	0.0648, 0.0704, 0.0465	0.0405, 0.0461, 0.0585	0.0088, 0.0160, 0.0071	0.0088, 0.0160, 0.0071	0.1361, 0.2272, 0.1516	0.2179, 0.3472, 0.1206
C		1–561	0.0464, 0.0705, 0.0543	0.0075, 0.0305, 0.0151	0.0119, 0.0095, 0.0143	0.0024, 0, 0.0047	0.2561, 0.1345, 0.2629	0.3132, 0, 0.3127
V	V trans[d]	690–902	0, 0.0217, 0.0439	0.0434, 0.0667, 0.0902	0.0063, 0, 0	0.0063, 0, 0	NA, 0, 0	0.1449, 0, 0
M		1–1008	0.0842, 0.0936, 0.0892	0.2135, 0.2134, 0.2141	0.0026, 0.0026, 0.0026	0.0758, 0.0758, 0.0772	0.0310, 0.0279, 0.0293	0.3551, 0.3552, 0.3606
F		1–1653	0.0566, 0.0627, 0.0675	0.0355, 0.0459, 0.0621	0, 0.0024, 0.0024	0.0089, 0.0113, 0.0113	0, 0.0359, 0.0357	0.2504, 0.2470, 0.1825
H		1–1854	0.0902, 0.0877, 0.0724	0.0675, 0.0651, 0.0907	0.0114, 0.0100, 0.0092	0.0085, 0.0071, 0.0135	0.1263, 0.1135, 0.1276	0.1262, 0.1089, 0.1490
L		1–6549	0.0801, 0.0927, 0.0822	0.0601, 0.0687, 0.0781	0.0047, 0.0051, 0.0049	0.0050, 0.0054, 0.0058	0.0584, 0.0548, 0.0594	0.0828, 0.0782, 0.0739

[a] Edwt, Edmonston wild type; IC(D3), IC-B; 9301(D5), 9301B; WA98(D6), WA.USA/17.98.
[b] The first nucleotide of the initiation codon for each open reading frame is taken as 1.
[c] NA, not applicable.
[d] V trans is the C-terminal region unique to the V protein.

a nonsense mutation at amino acid position 532 (Table 2). These changes in the F protein are typical of SSPE strains (4, 9, 31, 44). For the N, H, and L protein reading frames, in contrast, the Ka/K_s ratios revealed by the comparisons between the SI and clade D MV strains were similar to those observed between the Edmonston wt and clade D MV strains (Table 1). These data indicated that similar levels of stabilizing selection pressure operated for the N, H, and L protein reading frames of the SI strain during the persistent infection in the brain. For the P gene, it was not simple to assess the data for the Ka and K_s values, since the gene contains overlapping reading frames. Nonetheless, it was evident that both the C and V nonstructural proteins were highly conserved during the persistent infection in the brain. For the C protein-reading frame, the Ka values for the IC/SI and WA93/SI comparisons were as much as 3 to 5 times lower than those for the IC/Edwt and WA93/SI comparisons (Table 1). Indeed, no amino acid substitution was found in the C protein of the SI strain compared with that of the 9301B strain. Similarly, no amino acid substitution was found in the V protein-unique region of the SI strain compared with that of the WA.USA/17.98. strain. The V protein-unique region of the 9301B strain also had the same amino acid sequence as those of the SI and WA.USA/17/98 strains except that the 9301B V protein possessed an additional single amino acid at the carboxyl-terminal end, because it terminated one codon later (since this additional codon was not included in calculation, the Ka of 9301/SI comparison was zero [Table 1]). These data suggested that both the C and V proteins played important roles in the survival of the SI strain in the brain.

Generation of a recombinant SI strain expressing a fluorescent protein by establishment of an efficient MV rescue system. The SI strain did not produce cell-free infectious particles and spread poorly in cell cultures (data not shown). In addition, a CPE was barely detectable in some cultured cells, although the SI strain replicated in them (data not shown). Many studies have shown that the use of recombinant viruses genetically engineered to express a fluorescent protein is greatly advantageous for monitoring virus infections, especially when the virus infection shows a small or weak CPE. Therefore, we decided to generate a recombinant SI strain expressing a fluorescent protein. A full-length genome cDNA of the SI strain possessing an additional transcriptional unit encoding AcGFP between the H and L genes was generated and inserted into the pBluescript vector downstream of the T7 promoter (Fig. 2). The T7 promoter was followed by three guanines that enhance the transcription efficiency (Fig. 2). Since these guanines produce extra guanine residues at the 5′ end of the synthesized MV antig-

TABLE 2. Amino acid substitutions in the F proteins among the IC, SI, and Edmonston strains

Amino acid no.	Amino acid substitution(s) or category		
	IC	SI	Ed
78	R	G	R
165	R	K	R
167	A	T	A
187	I	V	I
242	I	T	I
246	L	F	L
247	E	K	E
268	G	D	G
300	E	G	E
487	M	I	M
532	R	Stop	R
533–550	18 aa[a]	Deletion	18 aa

[a] aa, amino acids.

Downloaded from http://jvi.asm.org/ on January 30, 2013 by NATL INST OF INFECTIOUS DISEAS

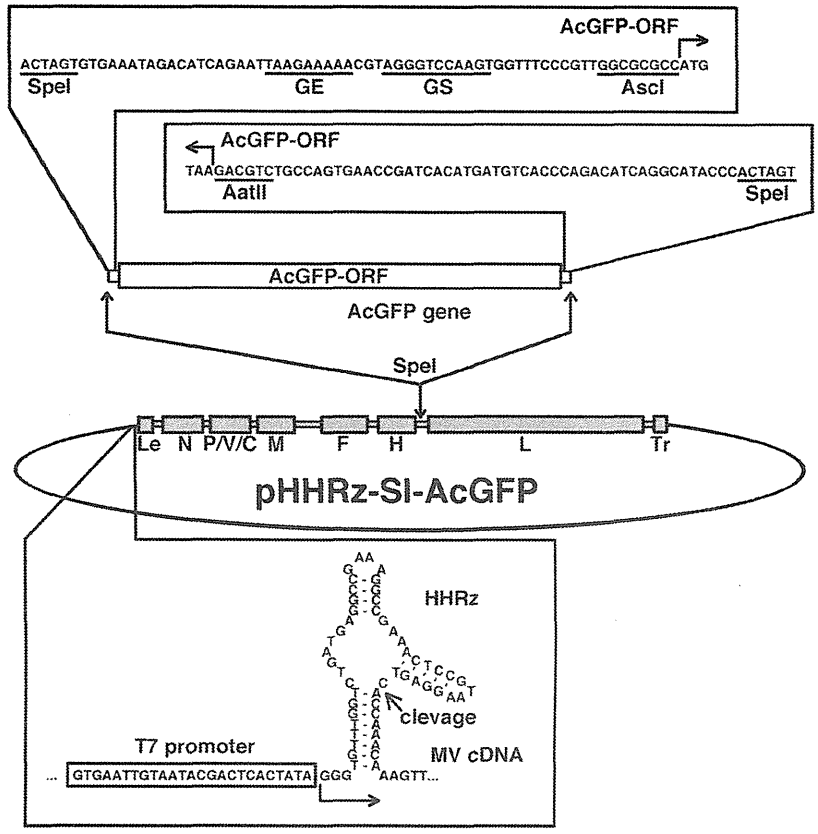

FIG. 2. Diagram of the genome plasmid with insertion of an additional transcriptional unit and the HHRz sequence. Transcriptional regulatory regions (gene end [GE], intergenic, and gene start [GS] sequences) and the coding sequence for AcGFP (AcGFP-ORF) were inserted at the junction between the H and L genes by the use of appropriate restriction enzyme recognition sites (SpeI, AscI, and AatII). The recombinant genome also possesses an HHRz upstream the authentic virus genome.

enome, a precise 5′ end for the MV antigenome was created by inserting HHRz between the three guanines and the first viral nucleotide (Fig. 2). The resulting full-length genome plasmid was designated pHHRz-SI-AcGFP. BHK/T7-9 cells, which represent a baby hamster kidney (BHK) cell-derived clone constitutively expressing T7 RNA polymerase (20) (kindly provided by M. Sugiyama and N. Ito), has been shown to be highly potent for initiating the replication cycles of other negative-strand RNA viruses from cloned cDNAs (20, 48). By the use of previously reported methods of studies employing BHK/T7-9 cells (48), the cDNAs of the N, P, and L genes of MV were inserted into the pCITE vector; the resulting plasmids were termed pCITE-IC-N, pCITE-IC-PΔC, and pCITEko-9301B-L, respectively. These plasmids were designed to create an internal ribosome entry site at the 5′ terminus of the N, P, and L mRNAs. Since the ratios of the plasmids expressing the N, P, and L proteins were previously reported to be critical for the initiation of infectious cycles of paramyxoviruses from cloned cDNAs (13, 21, 26), the optimal ratio for these plasmids was determined using a minireplicon assay for MV (23). The analyses indicated that 0.20, 0.15, and 0.40 μg of pCITE-IC-N, pCITE-IC-PΔC, and pCITEko-9301B-L, respectively, were optimal for the expression of the MV minireplicon gene (luciferase) in BHK/T7-9 cells cultured in a 24-well cluster plate (see Table S3 in the supplemental material). When BHK/T7-9 cells cultured in a 6-well cluster plate were transfected with 5.0 μg of pHHRz-SI-AcGFP together with three support plasmids (0.80, 0.60, and 1.60 μg of pCITE-IC-N, pCITE-IC-PΔC, and pCITEko-9301B-L, respectively), infectious cycles of rSI-AcGFP were efficiently initiated from pHHIRz-SI-AcGFP. Subsequently, the recombinant SI strain expressing AcGFP

TABLE 3. Detection of the M protein by an indirect immunofluorescence assay

MAb clone no.	Antigenic site	Assay result			
		IC323-AcGFP	SI-AcGFP	IC-M-mCherry	SI-M-mCherry
A23	II	+	−	+	−
A24	II	+	−	+	−
A27	II	+	−	+	−
A154	II	+	−	+	−
A157	II	+	−	+	−
A177	II	+	−	+	−
B46	II	+	−	+	−
A39	III	+	−	+	−
A41	III	+	−	+	−
A42	III	+	−	+	−
A51	III	+	−	+	−
A133	IV	+	−	+	−

Downloaded from http://jvi.asm.org/ on January 30, 2013 by NATL INST OF INFECTIOUS DISEAS

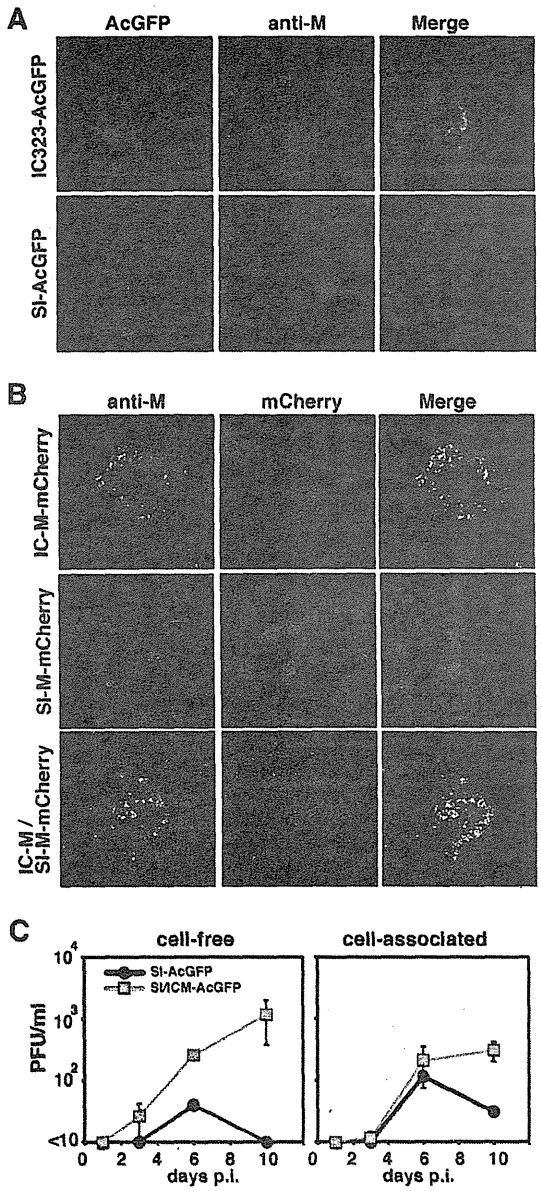

FIG. 3. Distribution of the M protein and effect on viral growth of strain SI possessing the IC-M gene. (A) Distribution of the M protein in cells infected with recombinant MV. Vero/hSLAM cells were infected with IC323-AcGFP or SI-AcGFP. At 2 (IC323-AcGFP) or 5 (SI-AcGFP) days postinfection, the cells were stained with an anti-M protein MAb (A42) and an Alexa Fluor 594-conjugated anti-mouse secondary antibody. The nuclei were stained with DAPI (blue). (B) Distribution of the mCherry-fused M protein. Vero/hSLAM cells were transfected with the M protein-expressing plasmids IC-M-mCherry, SI-M-mCherry, and IC-M plus SI-M-mCherry. At 1 day posttransfection, the cells were stained with an anti-M protein MAb (A42) and an Alexa 488-conjugated anti-mouse secondary antibody. The cells were observed under a confocal microscope. (C) Replication kinetics of recombinant MVs. Vero/hSLAM cells were infected with recombinant MVs at an MOI of 0.01, and infectious titers in culture medium (cell-free) and cells (cell-associated) were determined at 1, 3, 6, and 10 days p.i. Data represent the means ± standard deviations (SD) of results from triplicate samples.

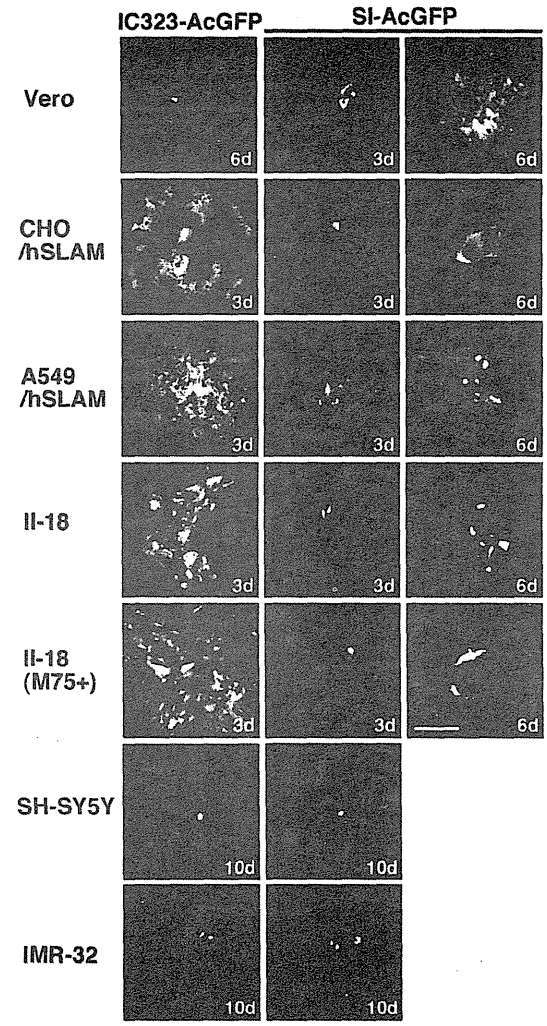

FIG. 4. AcGFP autofluorescence in cells infected with IC323-AcGFP and SI-AcGFP. Vero, CHO/hSLAM, A549/hSLAM, II-18, SH-SY5Y, and IMR-32 cells were infected with IC323-AcGFP or SI-AcGFP. Some II-18 cells were incubated with an anti-CD46 MAb (M75). The cells were observed under a fluorescence microscope at the indicated days (d). Bar, 0.20 mm.

(rSI-AcGFP) was maintained in Vero/hSLAM cells cocultured with BHK/T7-9 cells.

Properties of the M protein of the SI strain. Using various MAbs against the M protein (42), an indirect immunofluorescence assay was performed. A total of 12 MAbs that have been shown to recognize antigenic sites II, III, and IV of the M protein were used (42) (Table 3). A recombinant IC323 strain expressing AcGFP (IC323-AcGFP) was generated and used as a control. The IC323 strain is a recombinant MV based on the wt IC-B strain (60). In cells infected with IC323-AcGFP, all the MAbs detected the M protein (Fig. 3A and Table 3). However, in cells infected with the SI or rSI-AcGFP strains, all the MAbs failed to detect the M protein (Fig. 3A and Table 3 and data not shown). These data suggested a lack of M protein expression in cells infected with the SI and rSI-AcGFP strains. Sato et al. (43) also previously showed that M protein expression

Downloaded from http://jvi.asm.org/ on January 30, 2013 by NATL INST OF INFECTIOUS DISEAS